Supporting Information

Bing Liu, et al.

3

4

1

2

SI Materials and Methods

5

6 Model inputs for global simulations. Sixty locations from key wheat growing regions in the 7 world were used for a global impact assessment (Table S1). Locations 1 to 30 are high rainfall or 8 irrigated wheat growing locations representing 68% of current global wheat production. These 9 locations were simulated without water or nitrogen limitation. Details about these locations can be found in Asseng, et al. (1) and in Table S1. Locations 31 to 60 are low rainfall rainfed 10 locations with average wheat yield < 4 t ha⁻¹. These locations represent 32% of current global 11 wheat production. In contrast to the high-rainfall locations 1 to 30, soil types and N management 12 vary among the low-rainfall locations 31 to 60 according region-specific practices. 13 14 To carry out the global impact assessment and exclusively focus on climate change, regionspecific cultivars were used in all 60 locations. Observed local mean sowing, anthesis, and 15 maturity dates were supplied to modelers with qualitative information on vernalization 16 requirements and photoperiod sensitivity for each cultivar. Modelers were asked to sow at the 17 supplied sowing dates and calibrate their cultivar parameters against the observed anthesis and 18 19 maturity dates by considering the qualitative information on vernalization requirements and 20 photoperiod sensitivity. For locations 1 to 30 sowing dates were fixed at specific dates. For locations 31 to 60, sowing 21 22 windows were defined and a sowing rule was used. The sowing window was based on sowing 23 dates reported in literature (Table S1). For locations 41, 43, 46, 53, 54, and 59, sowing dates were not reported in literature and estimates from a global cropping calendar were used (2). The 24 cropping calendar provided a month (the 15th of the month was used) in which wheat is usually 25 26 sown in the region of the location. The start of the sowing window was the reported sowing date 27 and the end of the sowing window was set two months later. Sowing dates and windows are listed in Table S1. Sowing was triggered in the simulations on the day after cumulative rainfall 28 29 reached or exceeds 10 mm over a 5-day period during the predefined sowing window. Rainfall

- 1 from up to 5 days before the start of the sowing window was considered. If these criteria were
- 2 not met by the end of the sowing window, wheat was sown on the last day of the sowing
- 3 window.
- For locations 35, 39, 47, 49, and 55 to 57, anthesis dates were reported in literature. For the
- 5 remaining sites, anthesis dates were estimated with the APSIM-Wheat model.
- 6 Maturity dates were estimated from a cropping calendar for sites 31 to 32, 37 to 38, 41 to 46,
- 7 49 to 54, and 58 to 59 where no information from literature was available. For locations 31 to 60,
- 8 observed grain yields from the literature (Table S1) were provided to modelers with the aim to
- 9 set up wheat models to have similar yield levels, as well as similar anthesis and maturity dates.
- No yields were reported for sites 49 and 56, so APSIM-Wheat yields were estimated and used as
- 11 a guide.
- Locations 1 to 30 (no water or N limitations) were simulated using the same soil information
- from Maricopa, USA. Soil information for locations 31 to 60 were obtained from a global soil
- database (3). The soil closest to a location was used, but for locations 39 and 59, soil carbon was
- decreased after consulting local experts. Soil profile hydrological parameters and soil organic
- carbon used for locations 1 to 60.
- 17 Initial soil nitrogen was set to 25 kg N ha NO₃ and 5 kg N ha NH₄ per meter soil depth and
- reset each year for locations 31 to 60. Initial soil water for spring wheat sown after winter at
- locations 31 to 60 was set to 100 mm of plant available water, starting from 10 cm depth down to
- 20 100 mm was filled in between permanent welting point and field capacity. The first 10 cm were
- 21 kept at permanent welting point and reset each year. If wheat was sown after summer, initial soil
- water was set to 50 mm plant available water, starting from 10 cm depth down to 50 mm was
- 23 filled in between permanent welting point and field capacity. The first 10 cm were kept at the
- 24 permanent welting point and reset each year.
- For locations 31 to 60, fertilizer rates were determined from Gbegbelegbe, *et al.* (4) except for
- site 59 (Ethiopia) where N fertilizer was set to 60 kg N ha⁻¹. Fertilizer rates were set low (20 to
- 27 50 kg N ha⁻¹) at locations 31 to 32, 48, 51, 53, 60; medium (60 kg N ha⁻¹) at locations 33 to 43,
- 45 to 47, 49 to 50, 52, 54, 57 to 59; and relatively high (100 to 120 kg N ha⁻¹) at locations 44, 55
- 29 to 56. All fertilizer was applied at sowing.

- 1 **Crop Models.** Thirty-one wheat crop models (Table S2) within the Agricultural Model
- 2 Intercomparison and Improvement Project (AgMIP; www.agmip.org), were used for assessing
- 3 impacts of 1.5°C and 2.0°C global warming above pre-industrial time on global wheat
- 4 production. All model simulations were executed by the individual modeling groups with
- 5 expertise in using the model they executed.

- 7 Future climate projections. In this assessment, projections for 1.5 and 2.0°C global warming
- 8 scenarios were taken from five global climate models (GCMs) [MIROC5, NorESM1-M,
- 9 CanAM4 (HAPPI), CAM4-2degree (HAPPI), and HadAM3P], which were selected from the Half
- a degree Additional warming, Prognosis and Projected Impacts project (HAPPI; 5). The baseline
- 11 (1980-2010) climate data are from the AgMERRA climate dataset (6), which combines
- observations, data assimilation models, and satellite data products to provide daily maximum and
- minimum temperatures, solar radiation, precipitation, wind speed, vapor pressure, dew point
- temperatures, and relative humidity corresponding to the maximum temperature time of day for
- each location. Atmospheric carbon dioxide concentrations ([CO₂]) of 360, 423, and 487 ppm
- 16 CO₂ were used for baseline and 1.5 and 2.0°C global warming scenarios. There were 11
- treatments (baseline, five GCMs for 1.5, and five GCMs for 2.0 scenario) simulated for 60
- locations and 30 years:
- 19 1. Baseline (with 360ppm CO₂)
- 20 2. GCM MIROC5 (1.5°C with 423 ppm CO₂)
- 21 3. GCM NorESM1-M (1.5°C with 423 ppm CO₂)
- 4. GCM CanAM4 (HAPPI) (1.5°C with 423 ppm CO₂)
- 5. GCM CAM4-2degree (HAPPI) (1.5°C with 423 ppm CO₂)
- 24 6. GCM HadAM3P (1.5°C with 423 ppm CO₂)
- 25 7. GCM MIROC5 (2.0°C with 487 ppm CO₂)
- 8. GCM NorESM1-M (2.0°C with 487 ppm CO₂)
- 9. GCM CanAM4 (HAPPI) (2.0°C with 487 ppm CO₂)
- 28 10. GCM CAM4-2degree (HAPPI) (2.0°C with 487 ppm CO₂)
- 29 11. GCM HadAM3P (2.0°C with 487 ppm CO₂)

- 1 Climate scenarios. The impacts of temperature and CO₂ were further analyzed using a simple
- 2 delta method. Six treatments were simulated for the 60 global locations and 30 years of baseline
- 3 climate (1981-2010) with three temperature scenarios with main daily temperature increased by
- 4 0, 2, or 4°C factorized with two atmospheric CO₂ concentration, 360 (baseline) and 550 ppm.
- 5 The Baseline+2°C and Baseline+4°C scenarios were created by adjusting each day's maximum
- 6 and minimum temperatures upward by that amount and then adjusting vapor pressures and
- 7 related parameters to maintain the original relative humidity at the maximum temperature time of
- 8 day.

- 10 Aggregation of local climate change impacts to global wheat production impacts. Before
- aggregating local impacts at 60 locations to global impacts, we determined the actual production
- represented by each location following the procedure described by Asseng, et al. (1). The total
- wheat production for each country came from FAO country wheat production statistics for 2014
- 14 (www.fao.org). For each country, wheat production was classified into three categories (i.e., high
- rainfall, irrigated, and low rainfall). The ration for each category was quantified based on the
- Spatial Production Allocation Model (SPAM) dataset (https://harvestchoice.org/products/data).
- 17 For some countries where no data was available through the SPAM dataset, we estimated the
- 18 ratio for each category based on the country-level yield from FAO country wheat production
- 19 statistics. The high rainfall production and irrigated production in each country were represented
- by the nearest high rainfall and irrigated locations (locations 1 to 30). Low rainfall production in
- each country was represented by the nearest low rainfall locations (locations 31 to 60).
- The global wheat grain and protein production impact was calculated using the following
- 23 steps:
- 1) Calculate the relative simulated mean yield (or protein yield) impact for climate change
- scenarios for 30 years (1981-2010) per single model at each location.
- 26 2) Calculate the median across 31 models and five GCMs per location (multi-crop models
- [CMs] and GCMs ensemble median). Note that CMs and GCMs simulation results were
- 28 kept separate only for calculating the separate CM and GCM uncertainties (expressed as
- range between 25th and 75th percentiles).

- 3) Calculate the absolute regional production loss by multiplying the relative yield (or protein yield) loss from the multi-model ensemble median with the production represented at each location (using FAO country wheat production statistics of 2014 (7)). Calculate separately for high rainfall/irrigated and low input rainfed production. This assumes that the selected simulated location is representative of the entire wheat-growing region surrounding this location.
 - 4) Add all regional production losses to the total global loss.

- 5) Calculate the relative change in global production (i.e., global production loss divided by current global production).
- 6) Repeat the above steps for the 25th and 75th percentile relative global yield impact from the 31model ensemble.
- Similar steps with global impacts were used for calculating the impacts on country scale impacts, except that only the local impacts from corresponding locations in each country were aggregated to the country impacts. The upscaling method used has been shown to give similar temperature impacts than global-gridded and regression- model based approach (8, 9).

Environmental clustering of the 60 global locations. The 60 global wheat growing locations were clustered in order to analysis the results by group of environments with similar climates. A hierarchical clustering on principal components of the 60 locations was performed based on four climate variables for 1981-2010: the growing duration (sowing to maturity) mean temperature, the growing duration cumulative evapotranspiration, the growing duration cumulative solar radiation, and the number of heat stress days (maximum daily temperature > 32°C) during the grain filling period. All data were scaled (centered and reduced) prior to the principal component analysis.

Data analysis. All data were analyzed and plotted using the R language and environment for statistical analysis version 3.4.1 (10). The principal component and hierarchical clustering analyses were done with the R package FactoMineR (11).

Table S1. Details of the 60 locations used in this study

•	14.5	
Cu	ltiva	r

Location number	Country	Location	Latitude / longitude (decimal)	Elevation (m a.s.l)	Irrigation (Y/N)	Name	Growth habit ^a	Vernalization requirement	Photoperiod sensitivity ^b	Sowing date or window	Mean 50%- anthesis date	Mean maturity date	Reference used for choosing anthesis date	Environ ment type ^g
01	USA, NE	Maricopa	33.06 / -112.05	358	Υ	Yecora Rojo	S	2	1	25 Dec.	5 Apr.	15 May	-	3
02	Mexico	Obregon	27.33 / -109.9	41	Υ	Tacupeto C2001	S	2	2	1 Dec.	15 Feb.	30 Apr.	-	3
03	Mexico	Toluca	19.40 / -99.68	2,667	Υ	Tacupeto C2001	S	2	2	10 May	5 Aug.	20 Sep.	-	1
04	Brazil	Londrina	-23.31 / -51.13	610	Υ	Atilla	S	3	3	20 Apr.	10 Jul.	1 Sep.	-	2
05	Egypt	Aswan	24.10 / 32.90	193	Υ	Seri M 82	S	3	2	20 Nov.	20 Mar.	30 Apr.	-	3
06	The Sudan	Wad Medani	14.40 / 33.50	413	Υ	Debeira	S	3	2	20 Nov.	25 Jan.	25 Feb.	-	3
07	India	Dharwar	15.43 / 75.12	751	Υ	Debeira	S	3	2	25 Oct.	15 Jan.	25 Feb.	-	3
08	Bangladesh	Dinajpur	25.65 / 88.68	40	Υ	Kanchan	S	2	2	1 Dec.	15 Feb.	15 Mar.	-	3
09	The Netherland	Wageningen	51.97 / 5.63	12	N	Aminda	W	6	6	5 Nov.	25 Jun.	5 Aug.	-	1
10	Argentina	Balcarce	-37.75 / -58.3	122	N	Oasis	W	5	5	5 Aug.	25 Nov.	25 Dec.	-	3
11	India	Ludhiana	30.90 / 75.85	244	Υ	HD 2687	S	1	1	15 Nov.	5 Feb.	5 Apr.	-	3
12	India	Indore	22.72 / 75.86	58	Υ	HI 1544	S	0	1	25 Oct.	25 Jan.	25 Mar.	-	3
13	USA, WI	Madison	43.03 / -89.4	267	N	Brigadier	W	6	6	15 Sep.	15 Jun.	30 Jul.	-	1
14	USA, KS	Manhattan	39.14 / -96.63	316	N	Fuller	W	4	4	1 Oct.	15 May	01 Jul.	-	1
15	UK	Rothamsted	51.82 / -0.37	128	N	Avalon	W	3	3	15 Oct.	10 Jun.	20 Aug.	-	1
16	France	Estrées-Mons	49.88 / 3.00	87	N	Bermude	W	6	6	5 Oct.	31 May	15 Jul.	-	1
17	France	Orleans	47.83 / 1.91	116	N	Apache	W	5	4	20 Oct.	25 May	7 Jul.	-	1
18	Germany	Schleswig	54.53 / 9.55	13	N	Dekan	W	5	2	25 Sep.	15 Jun.	25 Jul.	-	1
19	China	Nanjing	32.03 / 118.48	13	N	NM13	W	4	4	5 Oct.	5 May	5 Jun.	-	1
20	China	Luancheng	37.53 / 114.41	54	Υ	SM15	W	6	4	5 Oct.	5 May	5 Jun.	-	1
21	China	Harbin	45.45 / 126.46	118	Υ	LM26	S	1	5	5 Apr.	15 Jun.	25 Jul.	-	3
22	Australia	Kojonup	-33.84 / 117.15	324	N	Wyallkatchem	S	2	4	15 May	5 Oct.	25 Nov.	-	3
23	Australia	Griffith	-34.17 / 146.03	193	Υ	Avocet	S	2	4	15 Jun.	15 Oct.	25 Nov.	-	3
24	Iran	Karaj	35.92 / 50.90	1,312	Υ	Pishtaz	S	2	2	1 Nov.	1 May	20 Jun.	-	1

Table S1. Continued

25	Pakistan	Faisalabad	31.42 / 73.12	192	Υ	Faisalabad-2008	S	0	2	15 Nov.	5 Mar.	5 Apr.	-	3
26	Kazakhstan	Karagandy	50.17 / 72.74	356	Υ	Steklov-24	S	2	4	20 May	1 Aug.	15 Sep.	-	1
27	Russia	Krasnodar	45.02 / 38.95	30	Υ	Brigadier	W	6	6	15 Sep.	20 May	10 Jul.	-	1
28	Ukraine	Poltava	49.37 / 33.17	161	Υ	Brigadier	W	6	6	15 Sep.	20 May	15 Jul.	-	1
29	Turkey	Izmir	38.60 / 27.06	14	Υ	Basri Bey	S	4	4	15 Nov.	1 May	1 Jun.	-	1
30	Canada	Lethbridge	49.70 / -112.83	904	Υ	AC Radiant	W	6	6	10 Sept.	10 Jun.	25 July.		1
31	Paraguay	Itapúa	-27.33 / -55.88	216	N	Based on Atilla	S	3	3	25 May – 25 Jul.	_ d	15 Oct. e	(12)	2
32	Argentina	Santa Rosa	-36.37 / -64.17	177	N	Based on Avocet	S	2	4	5 Jun. – 5 Aug.	_ d	15 Dec. ^e	(13)	2
33	USA, GA	Watkinsville	34.03 / -83.41	220	N	Based on Brigadier	W	6	6	25 Nov. – 25 Jan.	_ d	22 Jun.	(14)	3
34	USA, WA	Lind	47.00 / -118.56	522	N	Based on AC Radient	W	4	4	28 Aug. – 28 Oct.	_ d	31 Jul.	(15-17)	1
35	Canada	Swift Current	50.28 / -107.78	10	N	Based on Steklov-24	S	2	4	18 May. – 18 Jul.	16 Jul.	28 Aug.	(18)	2
36	Canada	Josephburg	53.7 / -113.06	631	N	Based on Steklov-24	S	2	4	15 May. – 15 Jul.	_ d	28 Aug.	(19)	2
37	Spain	Ventas Huelma	37.16 / -3.83	848	N	Based on Basri Bey	S	4	4	18 Dec. – 18 Feb.	_ d	15 Jun. ^e	(20)	2
38	Italy	Policoro	40.2 / 16.66	14	N	Based on Basri Bey	S	4	4	17 Nov. – 17 Jan.	_ d	15 May ^e	(21)	2
39	Italy	Libertinia	37.5 / 14.58	267	N	Based on Basri Bey	S	4	4	26 Nov. – 26 Jan.	4 May	30 May	(22)	1
40	Greece	Thessaloniki	41.08 / 22.15	36	N	Based on Basri Bey	S	4	4	15 Nov. – 15 Jan.	_ d	22 Jun.	(23)	1
41	Hungary	Martonvásár	47.35 / 18.81	113	N	Based on Apache	S	5	4	15 Nov. – 15 Jan. ^c	_ d	15 Jun. ^e	(24)	1
42	Romania	Alexandria	43.98 / 25.35	73	N	Based on Brigadier	W	6	6	7 Oct. – 7 Dec.	_ d	15 Aug. ^e	(25)	1
43	Bulgaria	Sadovo	42.13 / 24.93	154	N	Based on Brigadier	W	6	6	15 Oct. – 15 Dec. ^c	_ d	15 Jul. ^e	(26)	1
44	Finland	Jokioinen	60.80 / 23.48	107	N	Based on Steklov-24	S	2	2	1 May – 1 Jul.	_ d	15 Aug. ^e	(27)	2
45	Russia	Yershov	51.36 / 48.26	102	N	Based on Steklov-24	S	2	4	6 May – 6 Jul.	_ d	15 Sep. ^e	(28)	2
46	Kazakhstan	Altbasar	52.33 / 68.58	289	N	Based on Steklov-24	S	2	4	15 Mar. – 15 May ^c	_ d	15 Sep. ^e	(28)	2
47	Uzbekistan	Samarkand	39.70 / 66.98	742	N	Based on SM15	W	6	4	5 Nov. – 5 Jan.	7 May	5 Jul.	(29)	2
48	Morocco	Sidi El Aydi /	33.07 / -7.00	648	N	Based on Yecora	S	1	1	5 Nov. – 5 Jan.	_ d	1 Jun.	(30)	
		Jemaa Riah												2
49	Tunisia	Nabeul / Tunis	36.75 / 10.75	167	N	Based on Pishtaz	S	2	2	1 Dec. – 1 Feb.	29 Mar.	15 Jun. ^e	(31)	2
50	Syria	Tel Hadya /	36.01 / 36.56	263	N	Based on Pishtaz	S	2	2	20 Nov. – 20 Jan.	_ d	15 Jun. ^e	(32)	
		Aleppo												2
51	Iran	Maragheh	37.38 / 46.23	1,472	N	Based on SM15	W	6	4	13 Oct. – 13 Dec.	_ d	15 Jun. ^e	(33)	1
52	Turkey	Ankara	39.92 / 32.85	895	N	Based on Fuller	W	4	4	1 Sep. – 1 Nov	_ d	15 Jul. ^e	(34)	1
53	Iran	Ghoochan /	37.66 / 58.50	1,555	N	Based on Pishtaz	S	2	2	15 Oct. – 15 Dec. ^c	_ d	15 Jun. ^e	(35)	
		Quchan												1
54	Pakistan	Urmar	34.00 / 71.55	340	N	Based on Yecora	S	1	1	15 Nov. – 15 Jan. ^c	_ d	15 May	(36)	2
55	China	Dingxi	35.46 / 104.73	2,009	N	Based on Pishtaz	S	2	2	15 Mar. – 15 May.	15 Jun.	2 Aug.	(37)	2

Tah	ما	C1	Continued
ıav	16	J 1.	Continueu

56	China	Xuchang	34.01 / 113.51	110	N	Based on Wenmai	W	4	4	10 Oct. – 10 Dec.	25 Apr.	1 Jun.	f	2
57	Australia	Merredin	-31.50 / 118.2	3000	N	Based on Wyalkatchem	S	2	4	15 May – 25 Jul.	5 Oct.	25 Nov.	(38)	2
58	Australia	Rupanyup /	-37.00 / 143.00	219	N	Based on Avocet	S	2	4	1 May – 1 Jul.	_ d	15 Nov. e	(39)	
		Wimmera												2
59	Ethiopia	Adi Gudom	13.25 / 39.51	2,090	N	Based on Debeira	S	2	4	15 Jun. – 15 Aug. ^c	_ d	15 Dec. ^e	(40)	1
60	South Africa	Glen /	-28.95 / 26.33	1,290	N	Based on Wyalkatchem	S	2	4	15 May – 15 Jul.	_ d	15 Nov.	(41)	
		Bloemfontein												2

Location, name and characteristics of the cultivars, sowing date (locations 1-30) or sowing window (locations (31-60), and mean anthesis and physiological maturity date for the 30 locations (1-30) from high rainfall or irrigated wheat regions and thirty locations from low rainfall (low input) regions (31-60) of the world used in this study.

^a S, spring type; W, winter type.

^b Vernalization requirement and photoperiod sensitivity of the cultivars range from nil (0) to high (6).

^c Sowing date estimated using global cropping calendar.

^d See Figure S2.

^e Maturity date estimated using global cropping calendar.

f Yan Zhu, personal communication, August 4, 2015.

g 1, 2, 3 in environment type indicated temperate high rainfall, moderately hot low rainfall, and hot irrigated, respectively.

Table S2. List of the 31 wheat crop models used in the AgMIP Wheat study

Code	Name (version)	Reference	Documentation
AE	APSIM-E	(42-44)	http://www.apsim.info/Wiki
AF	AFRCWHEAT2	(45-47)	Request from John Porter: jrp@plen.ku.dk
AQ	AQUACROP (V.4.0)	(48)	http://www.fao.org/nr/water/aquacrop.html
AW	APSIM-Wheat (V.7.3)	(42)	http://www.apsim.info/Wiki
CS	CropSyst (V.3.04.08)	(49)	http://modeling.bsyse.wsu.edu/CS_Suite_4/CropSyst/index.html
DC	DSSAT-CERES-Wheat (V.4.0.1.0)	(50-52)	http://dssat.net/
DN	DSSAT-Nwheat	(53, 54)	http://dssat.net/
DR	DSSAT-CROPSIM (V4.5.1.013)	(51, 55)	http://dssat.net/
EI	EPIC-I (V0810)	(56-60)	http://epicapex.tamu.edu/epic
EW	EPIC-Wheat(V1102)	(56-58, 61, 62)	http://epicapex.brc.tamus.edu
GL	GLAM (V.2 updated)	(63, 64)	https://www.see.leeds.ac.uk/research/icas/research-
			themes/climate-change-and-impacts/climate-impacts/glam
HE	HERMES (V.4.26)	(65, 66)	http://www.zalf.de/en/forschung/institute/lsa/forschung/oekomod/hermes
IC	INFOCROP (V.1)	(67)	http://infocrop.iari.res.in/wheatmodel/UserInterface/HomeModule/Default.aspx
LI	LINTUL4 (V.1)	(68, 69)	http://models.pps.wur.nl/node/950
L5	SIMPLACE <lintul-5 canopyt,heatstresshourly<="" slimwater3,fao-56,="" td=""><td>(68-71)</td><td>http://www.simplace.net/Joomla/</td></lintul-5>	(68-71)	http://www.simplace.net/Joomla/
LP	LPJmL (V3.2)	(72-77)	http://www.pik-potsdam.de/research/projects/lpjweb
MC	MCWLA-Wheat (V.2.0)	(78-81)	Request from taofl@igsnrr.ac.cn
MO	MONICA (V.1.0)	(82)	http://monica.agrosystem-models.com
NC	Expert-N (V3.0.10) – CERES (V2.0)	(83-86)	http://www.helmholtz-muenchen.de/en/iboe/expertn
NG	Expert-N (V3.0.10) – GECROS (V1.0)	(85, 86)	http://www.helmholtz-muenchen.de/en/iboe/expertn
NP	Expert-N (V3.0.10) – SPASS (2.0)	(83, 85-88)	http://www.helmholtz-muenchen.de/en/iboe/expertn
NS	Expert-N (V3.0.10) – SUCROS (V2)	(83, 85, 86, 89)	http://www.helmholtz-muenchen.de/en/iboe/expertn
OL	OLEARY (V.8)	(90-93)	Request from gjoleary@yahoo.com
S2	Sirius (V2014)	(94-97)	http://www.rothamsted.ac.uk/mas-models/sirius.php
SA	SALUS (V.1.0)	(98, 99)	http://salusmodel.glg.msu.edu
SP	SIMPLACE <lintul-2 CC,Heat,CanopyT,Re-Translocation</lintul-2 	(100)	http://www.simplace.net/Joomla/
SQ	SiriusQuality (V3.0)	(101-105)	http://www1.clermont.inra.fr/siriusquality
SS	SSM-Wheat	(106)	Request from afshin.soltani@gmail.com
ST	STICS (V.1.1)	(107, 108)	http://www6.paca.inra.fr/stics_eng
WG	WheatGrow (V3.1)	(109-115)	Request from yanzhu@njau.edu.cn
WO	WOFOST (V.7.1)	(116)	http://www.wofost.wur.nl

Table S3. Variability of simulated grain yields for different environments under baseline, 1.5°C and 2.0°C warming scenarios

Coefficient of variation (%) Model GCM Type of environment Location Year Scenario 22.4 All locations Baseline 56.1 1.5 1.5°C HAPPI 55.4 1.6 22.7 1.1 2.0°C HAPPI 1.2 55.4 1.6 23.3 Temperate high Baseline 47.9 1.6 23.7 rainfall or irrigated 1.5°C HAPPI 46.4 1.7 23.3 1.2 2.0°C HAPPI 46.1 1.7 23.9 1.3 27.7 Moderately hot low 37.8 5.3 Baseline rainfall 1.5°C HAPPI 37.0 28.1 1.9 5.4 2.0°C HAPPI 5.5 28.7 1.9 36.9 Hot irrigated 26.5 2.7 27.8 Baseline 1.5°C HAPPI 27.1 2.8 28.5 0.6 2.0°C HAPPI 27.4 2.9 29.2 0.9

Variability due to location was calculated as coefficient of variation (CV) of simulated grain yields for corresponding locations (mean of 30 years, 31 models, and five global climate models [GCMs]). Variability due to year was calculated as CVs of simulated grain yields for 31 years (mean of corresponding locations, 31 models, and five GCMs). Variability due to model was calculated as CVs of simulated grain yields for 31 locations (mean of 30 years, corresponding locations and five GCMs). Variability due to GCM was calculated as CVs of simulated grain yields for five GCMs (mean of 30 years, 31 models and corresponding locations).

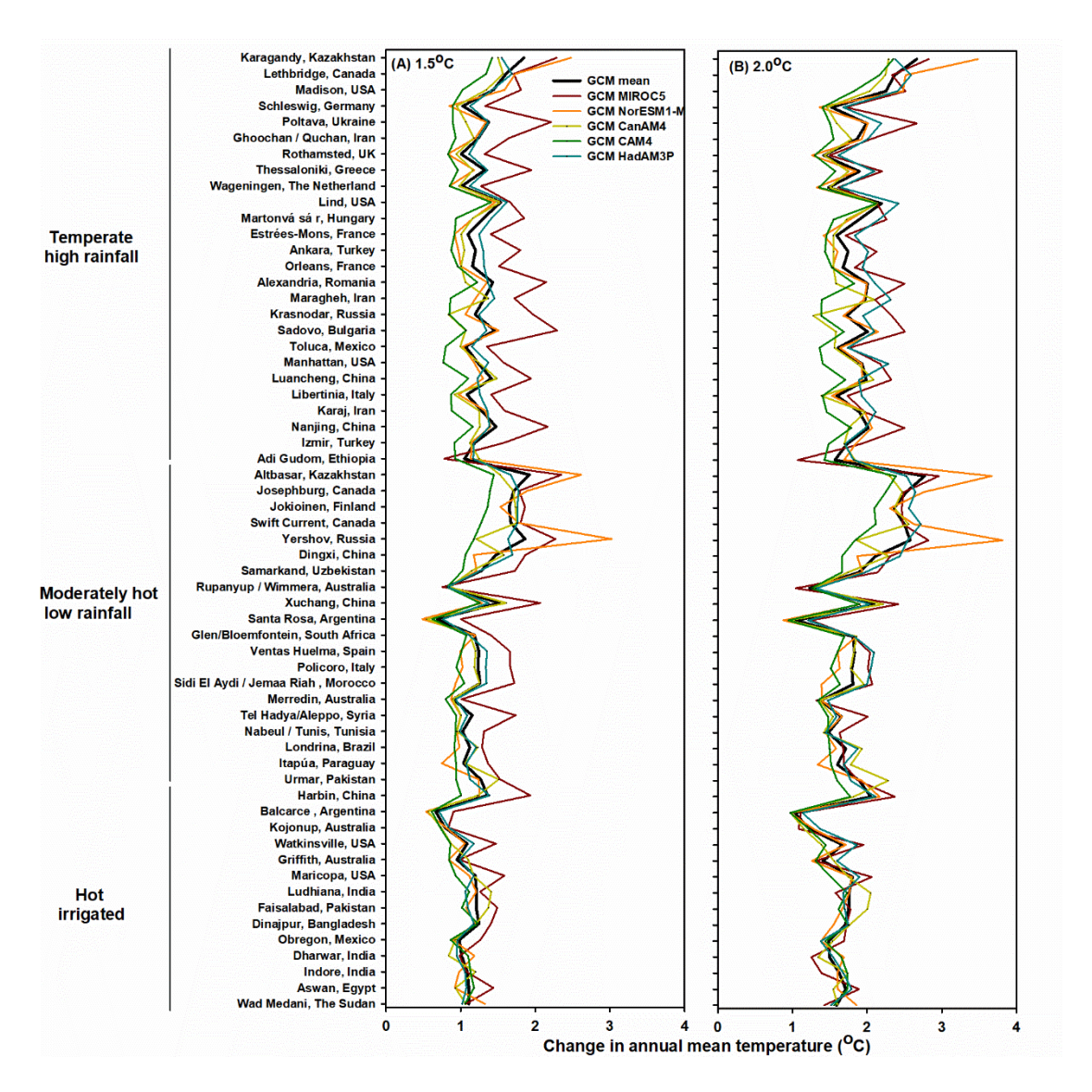


Fig. S1. Projected changes in annual mean temperature with the five global climate models (GCMs) for the 60 representative global wheat growing locations under (A) 1.5 and (B) 2.0 scenarios (HAPPI). The locations in each environment type were ordered by the annual mean temperature for the baseline period.

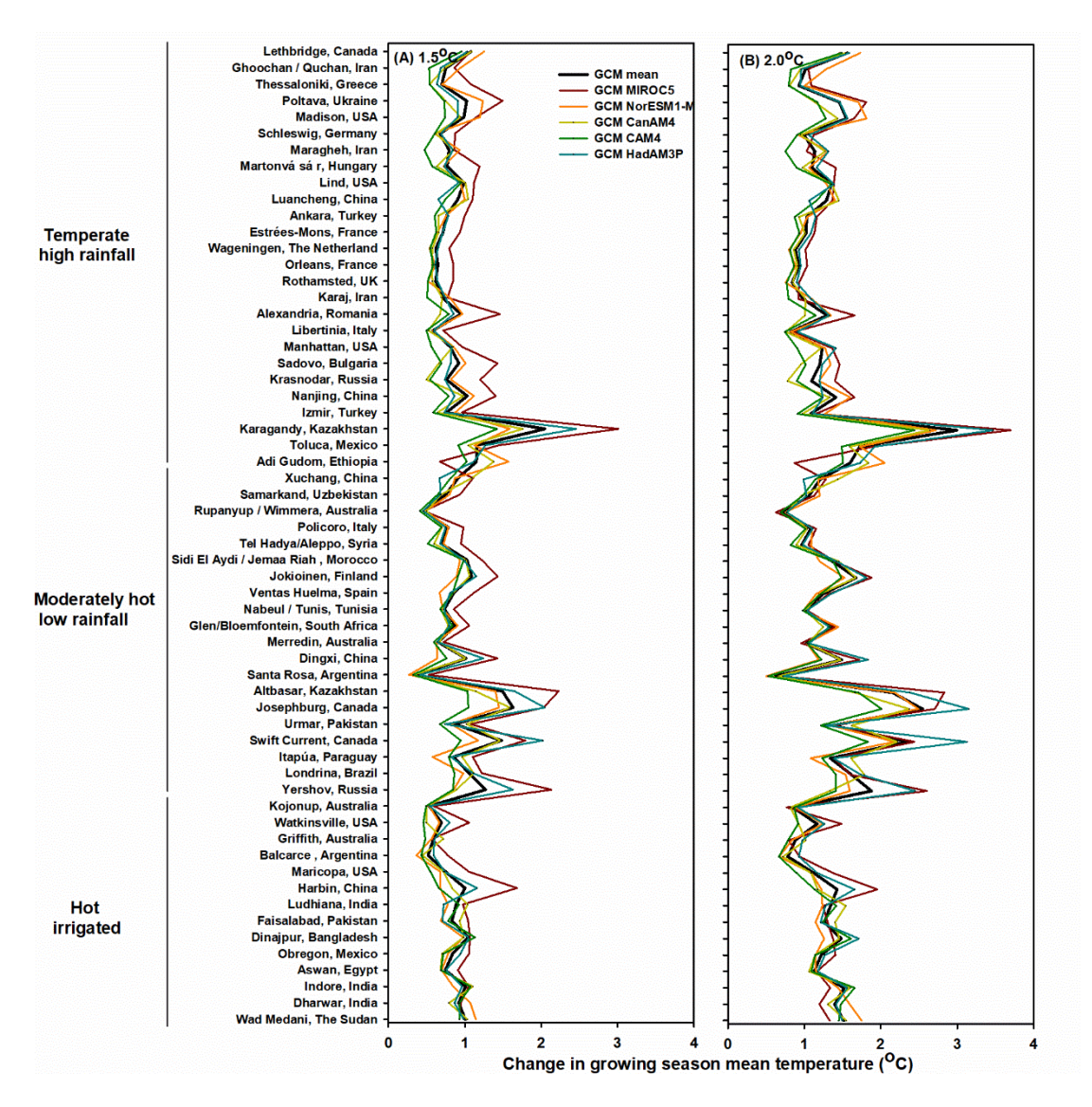


Fig. S2. Projected changes in growing season (sowing to maturity) mean temperature with the five global climate models (GCMs) for the 60 representative global wheat growing locations under (A) 1.5 and (B) 2.0 scenarios (HAPPI). The locations in each environment type were ordered by the growing season mean temperature for the baseline period.

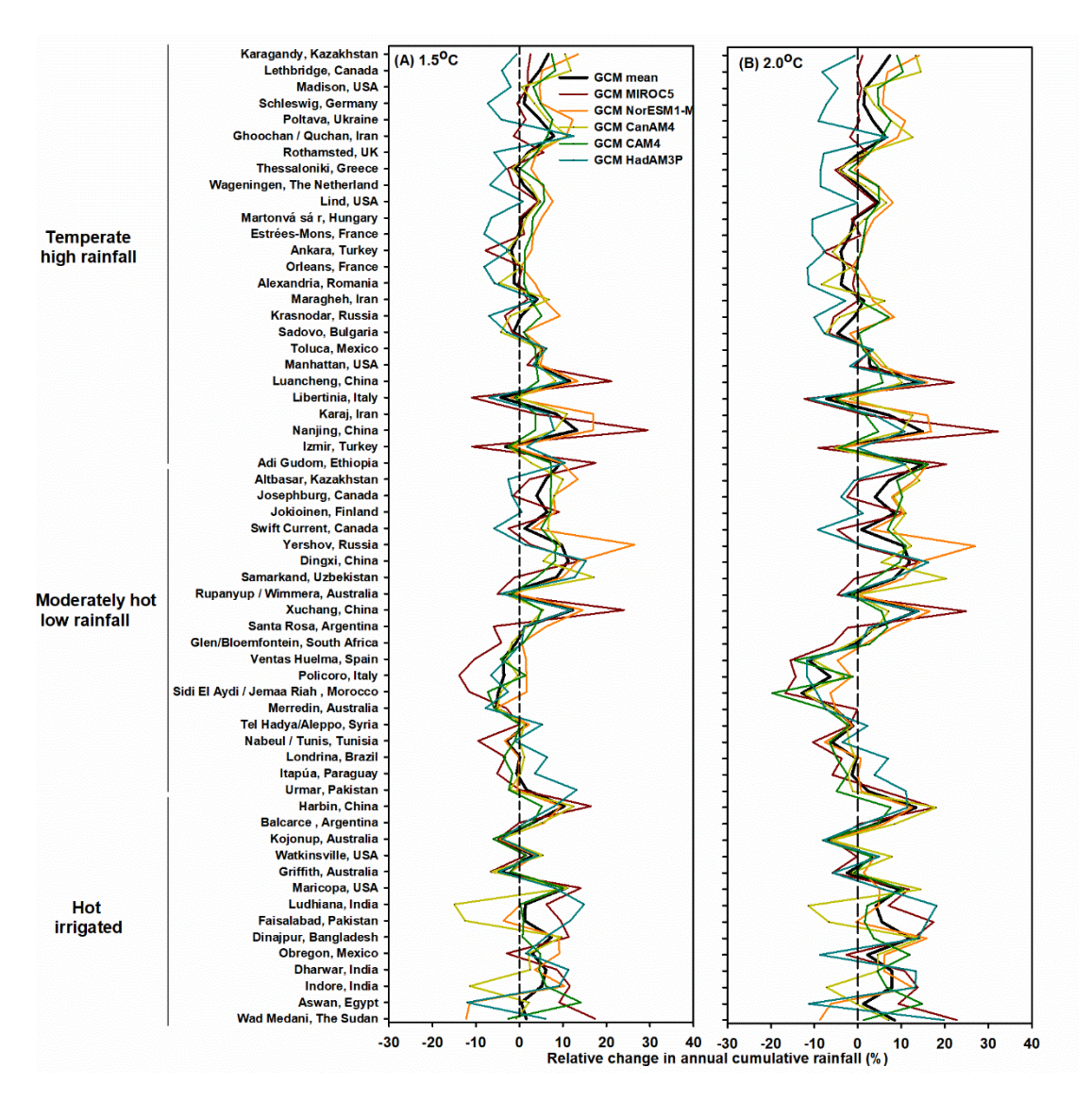


Fig. S3. Projected relative changes in annual cumulative rainfall with the five global climate models (GCMs) for the 60 representative global wheat growing locations under (A) 1.5 and (B) 2.0 scenarios (HAPPI). The locations in each environment type were ordered by the annual mean temperature for the baseline period.

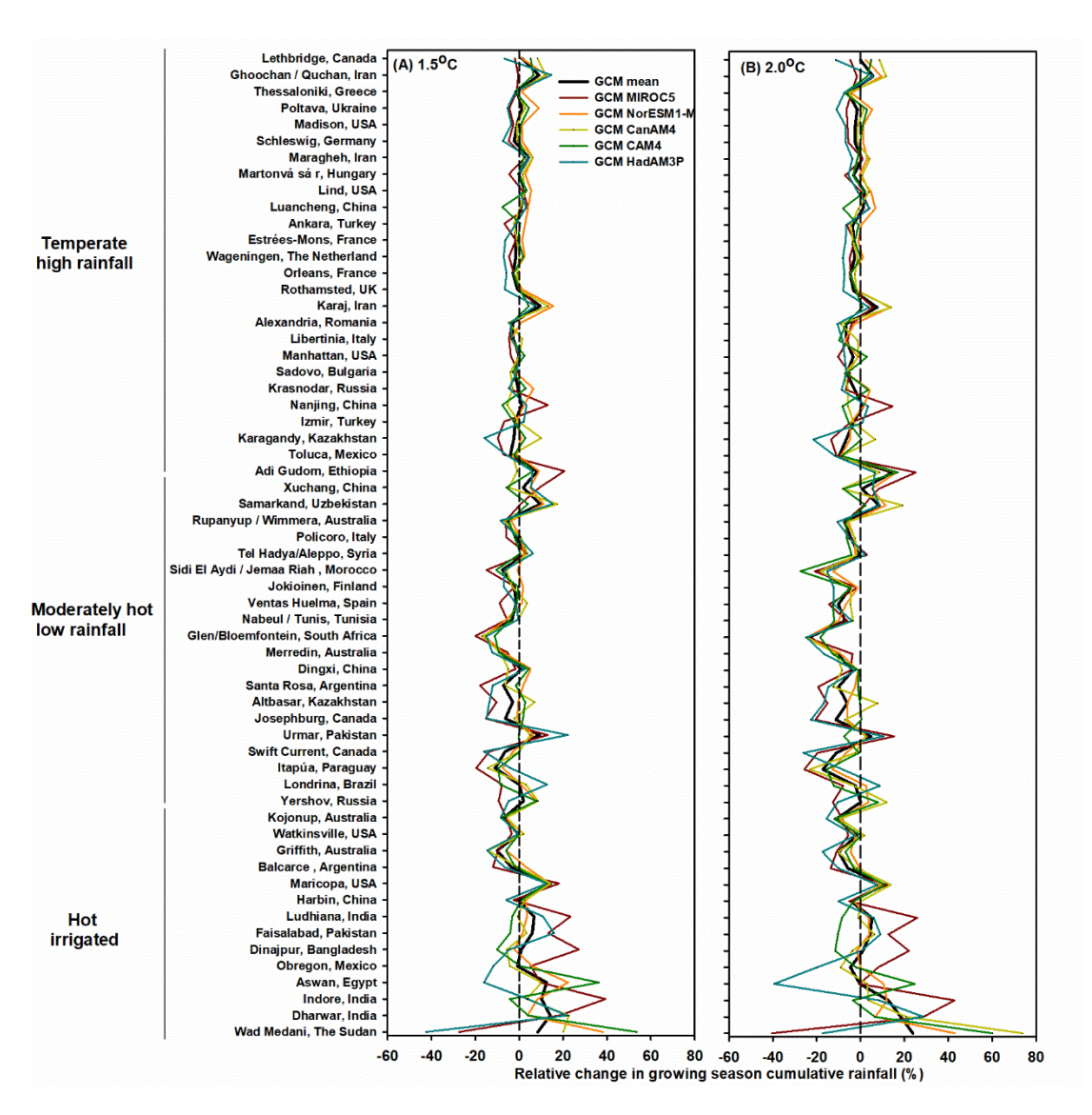


Fig. S4. Projected relative changes in growing season (sowing to maturity) cumulative rainfall with the five global climate models (GCMs) for the 60 representative global wheat growing locations under (A) 1.5 and (B) 2.0 scenarios (HAPPI). The locations in each environment type were ordered by the growing season mean temperature for the baseline period.

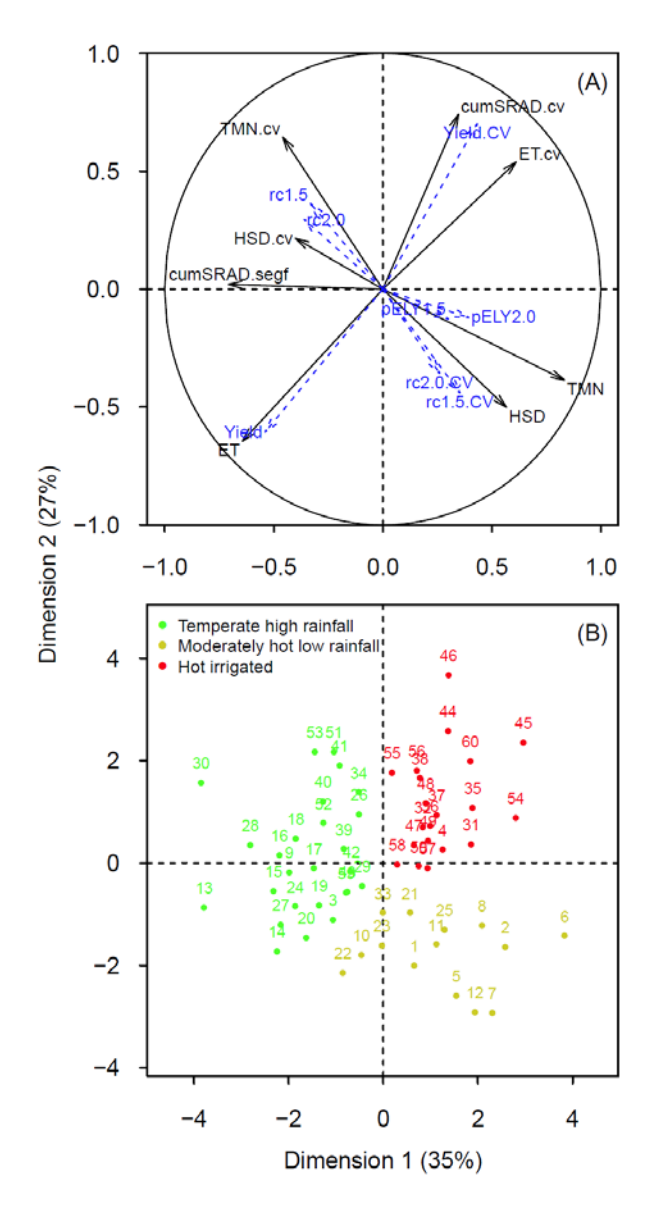


Fig. S5. Hierarchical clustering on principal components of 60 representative global wheat growing locations based on climate variables for 1981-2010. (A) Individual factor map with 30-years average and coefficient of variation for four climate variables (TMN, growing season [sowing to maturity] mean temperature; ET, growing season cumulative evapotranspiration; SRAD, growing season cumulative solar radiation; HSD, number of heat stress days [maximum daily temperature > 32°C] during the grain filling period). Blue, variables (Yield, average yield for the 1981-2010 baseline; Yield.cv, interannual yield variability [coefficient of variation] of yield for the 1981-2010 baseline; rc1.5 and rc2.0, relative changes in average yield for the 1.5 and 2.0 scenarios [HAPPI], respectively; rc1.5.CV and rc2.0.CV, relative changes in interannual yield variability for the 1.5 and 2.0°C warming scenarios, respectively; and pELY1.5 and pELY2.0, probabilities of extreme low yield [< 5% of baseline yield distribution] under the 1.5 and 2.0 scenarios, respectively) projected onto the same factorial plan but not used to construct the axes. (**B**) Location/cluster map of the principal component analysis. The numbers refer to the location ID given in Table S1.

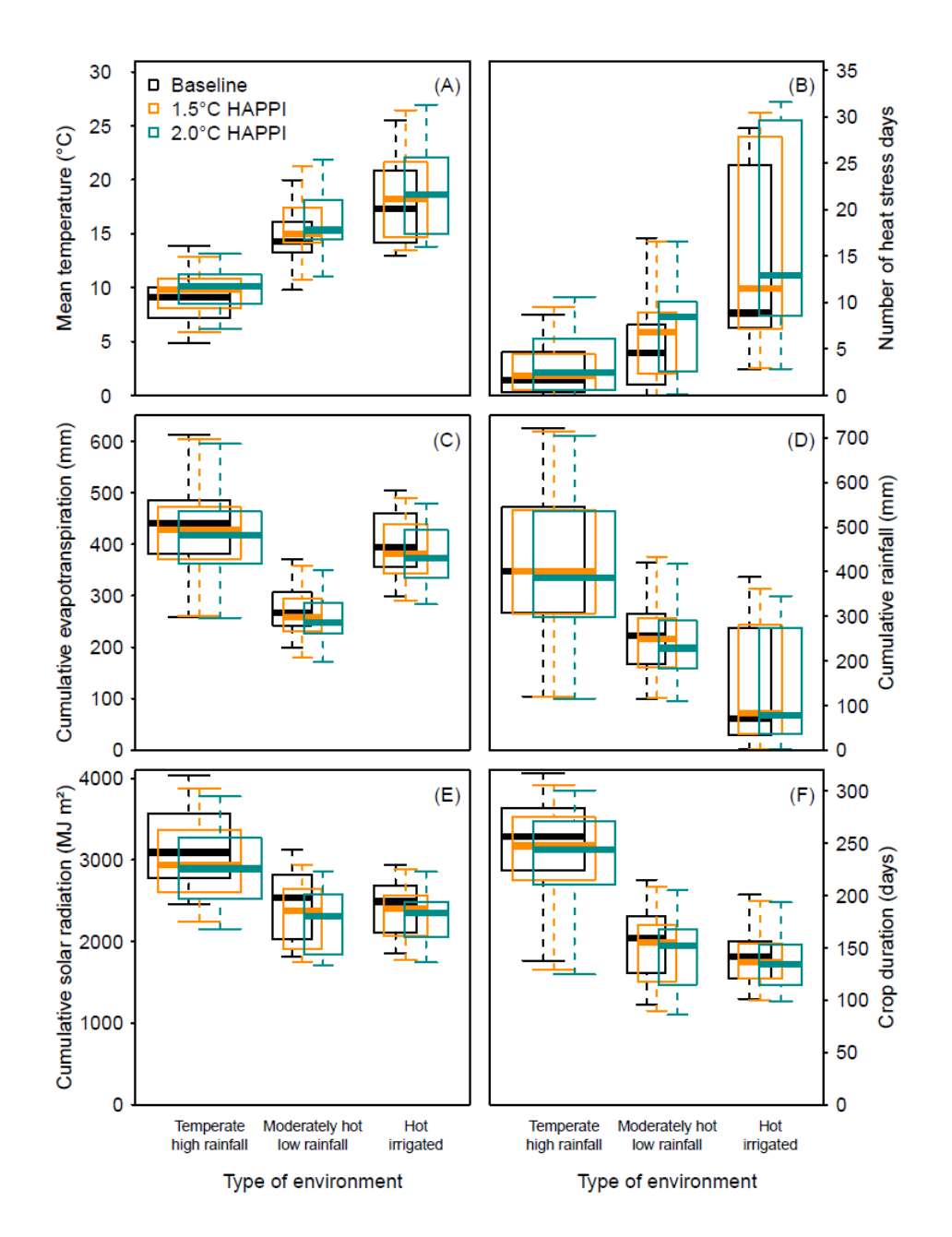


Fig. S6. Weather variables during wheat growing season (sowing to maturity) and crop duration in the three main types of environments for the 1981-2010 baseline and under 1.5 and 2.0 scenario. (A) Growing season mean temperature, (**B**) Number of heat stress days (maximum daily temperature > 32°C) during the post-flowering period. (**C**) Cumulative growing season evapotranspiration. (**D**) Cumulative growing season rainfall. (**E**) Cumulative growing season solar radiation. (**F**) Growing season duration. The width of the boxes is proportional to the percentage of global wheat production of each type of environment. The 60 global locations where clustered using 30-year means and coefficient of variability of the weather variables shown in this Figure S10. In each box plot, horizontal lines represent, from top to bottom, the 10th percentile, 25th percentile, median, 75th percentile and 90th percentile. In hot irrigated locations, growing season rainfall does not include the irrigation amount.

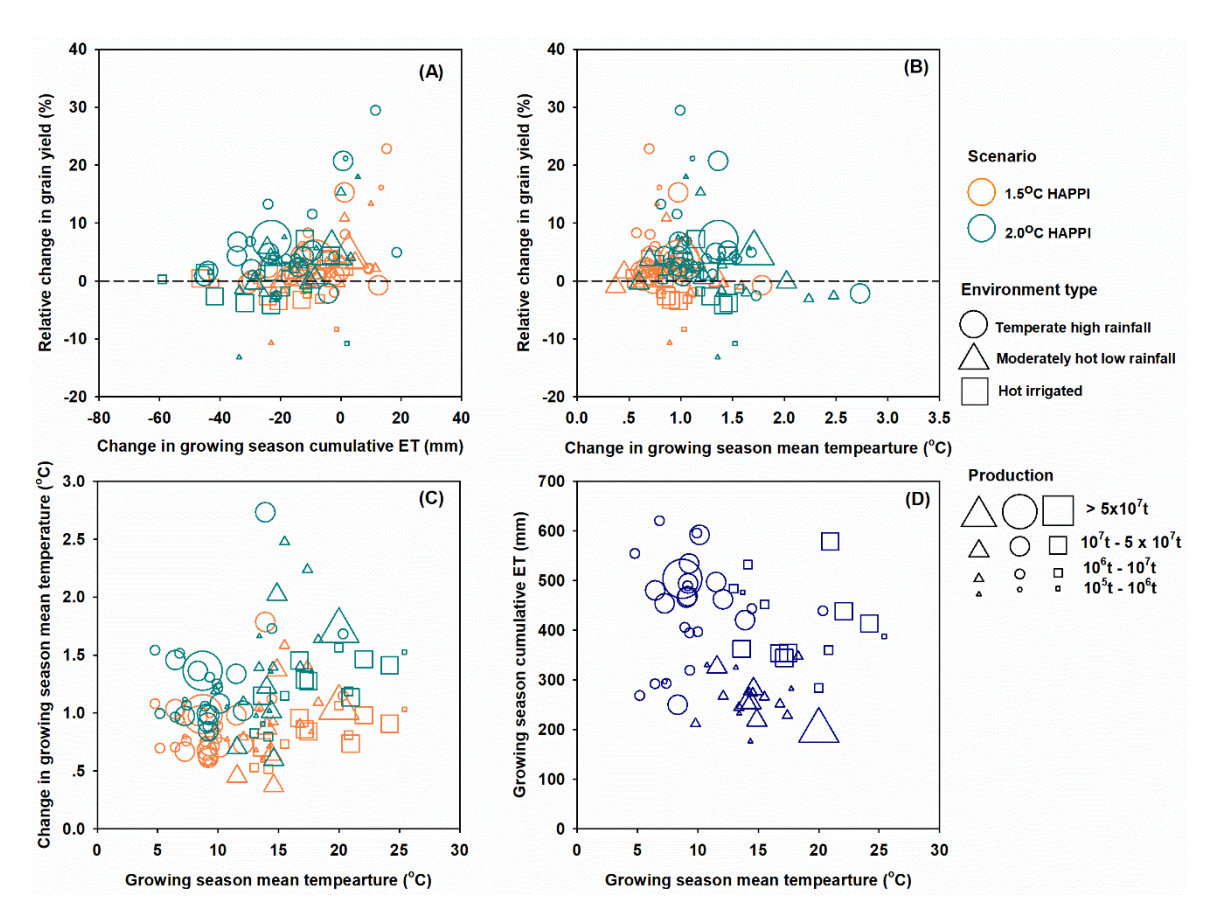


Fig. S7. Impact of 1.5 and 2.0 scenario on wheat grain yield, cumulative evapotranspiration (ET) and mean temperature. (A) Simulated change in grain yield versus baseline growing season (sowing to maturity) ET, (B) baseline growing season mean temperature. (C) Simulated change in growing season temperature and baseline growing season mean temperature under 1.5 (orange) and 2.0 (dark cyan) scenarios (HAPPI) and (D) Simulated baseline growing season ET and baseline growing season mean temperature for 60 representative global wheat growing locations. Relative changes of grain yield were the median across 31 crop models and five GCMs, calculated with simulated 30-year mean grain yields for baseline, 1.5 and 2.0 scenarios (HAPPI), including changes in temperature, rainfall, and atmospheric CO₂ concentration, using region-specific soils, cultivars and crop management. The size of symbols indicates the production represented at each location (using FAO country wheat production statistics). Growing season temperature is the mean of 30 years during baseline period (1981-2010) and the median across 31 crop models and five GCMs.

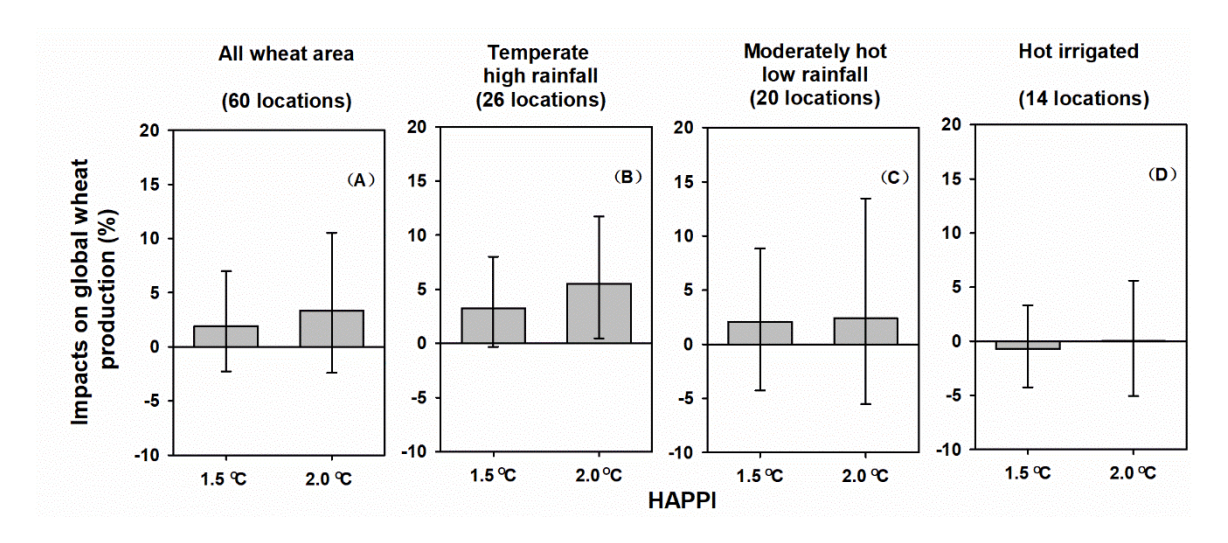
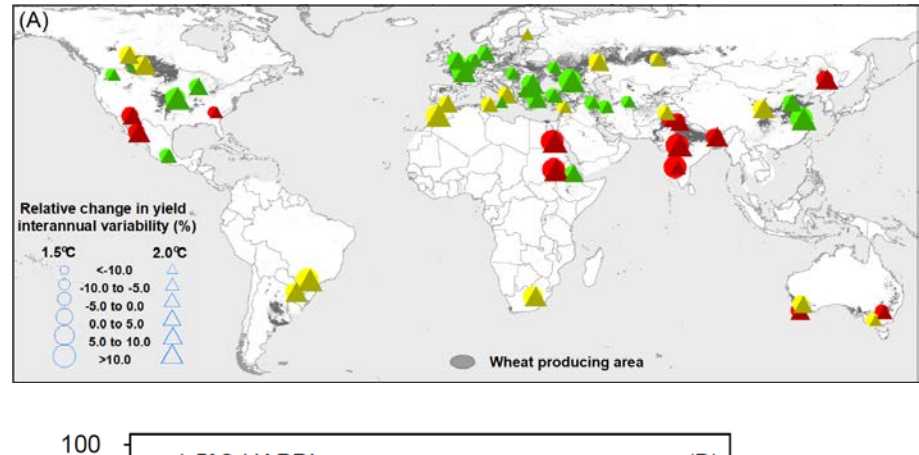


Fig. S8. Simulated global impacts of climate change under 1.5 and 2.0 scenario on wheat production from different environments. (A) All wheat area (60 locations). (B) Temperate high rainfall environment (26 locations). (C) Moderately hot low rainfall environment (20 locations). (D) Hot irrigated environment (14 locations). Impacts from the 60 global locations were weighted by FAO production area. Bars are ensemble median of 31 crop models and five GCMs for 1.5 and 2.0 scenarios (HAPPI), including changes in temperature, rainfall and atmospheric CO₂ concentration, and mean of 30 years using region-specific soils, cultivars, and crop management. Error bars indicate the 25th and 75th percentiles across 31 crop models and five GCMs.





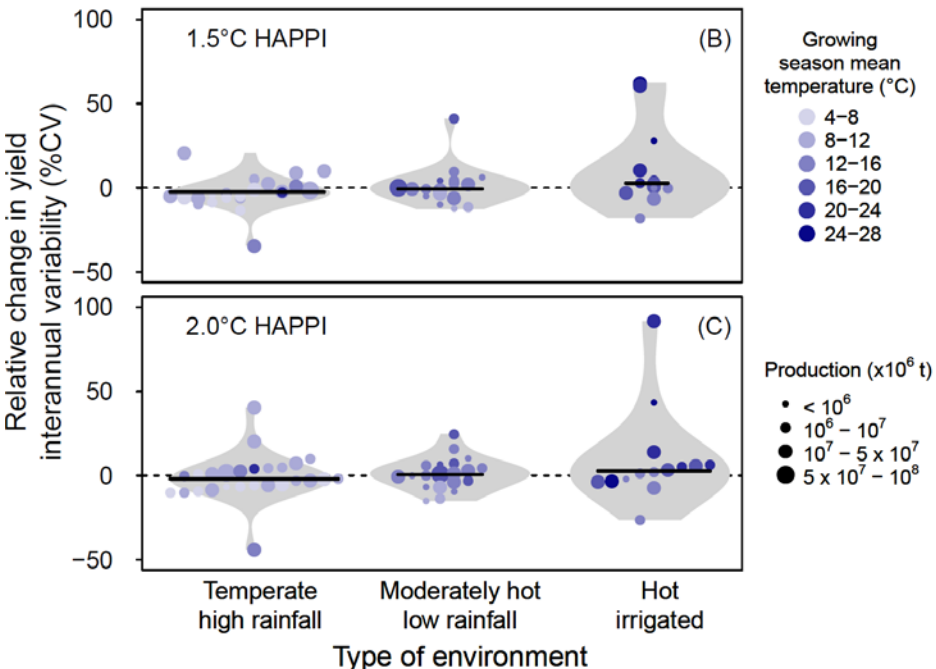


Fig. S9. Projected impacts of 1.5 and 2.0 scenario on wheat yield interannual variability. (A) Relative climate change impacts for the 1.5°C (circles) and 2.0°C (triangles) warming scenarios (HAPPI) compared with the 1981-2010 baseline on interannual yield variability (coefficient of variation) at 60 global locations. **(B)** and **(C)** Relative climate change impacts for the 1.5 and 2.0 scenarios compared with the 1981-2010 baseline on interannual yield variability (coefficient of variation) in temperate high rainfall or irrigated (26 locations), moderately hot low rainfall (20 locations), and hot irrigated (14 locations) environments. Horizontal thick solid lines are the median change of interannual yield variability for each environment type. The circles are the 60 global locations shown in (A), their size indicates the production represented at each location (using FAO country wheat production statistics) and their color the growing season mean temperature at each location under the 1.5 and 2.0 scenarios. Within each environment type the circles have been jiggled along the horizontal axis to make it easier to see locations with similar probability values. The shaded areas show the distribution of the data.

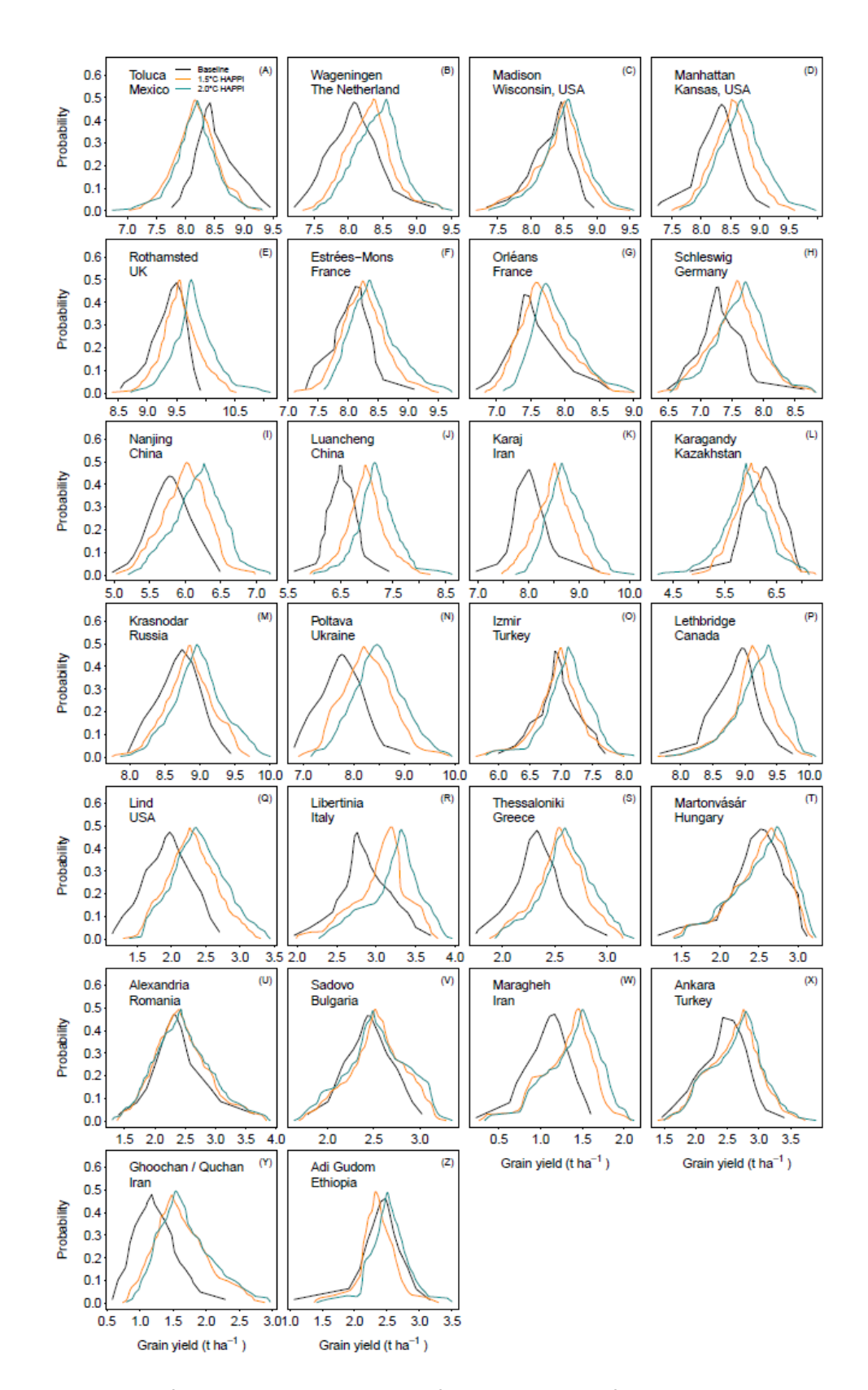


Fig. S10. Yield distribution for the 26 temperate high rainfall global locations for the 1981-2010 baseline and under 1.5 and 2.0 scenarios (including changes in temperature, rainfall and atmospheric CO₂ concentration).

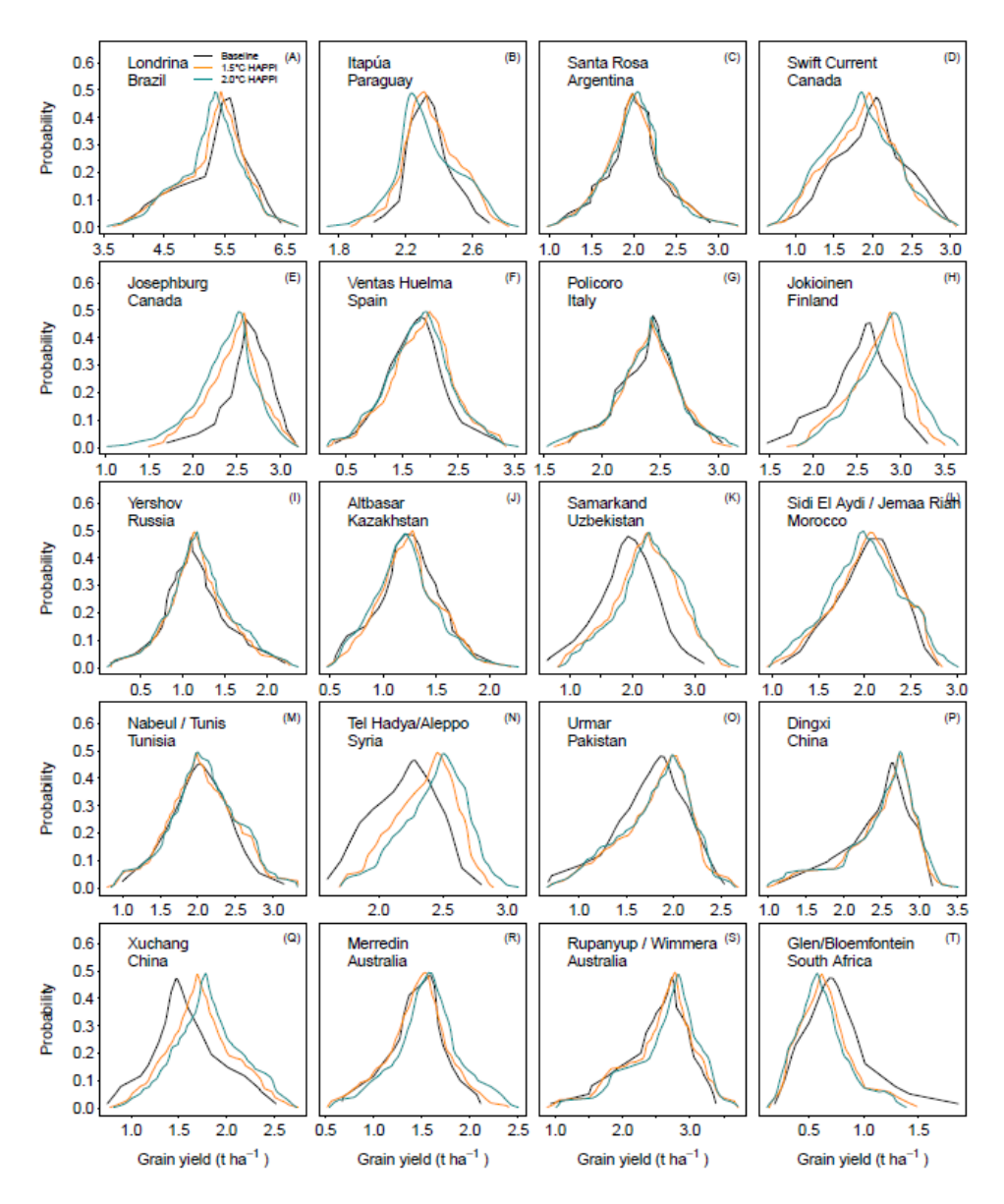


Fig. S11. Yield distribution at 20 moderately hot low rainfall global locations for the 1981-2010 baseline and under 1.5 and 2.0 scenarios (including changes in temperature, rainfall and atmospheric CO₂ concentration).

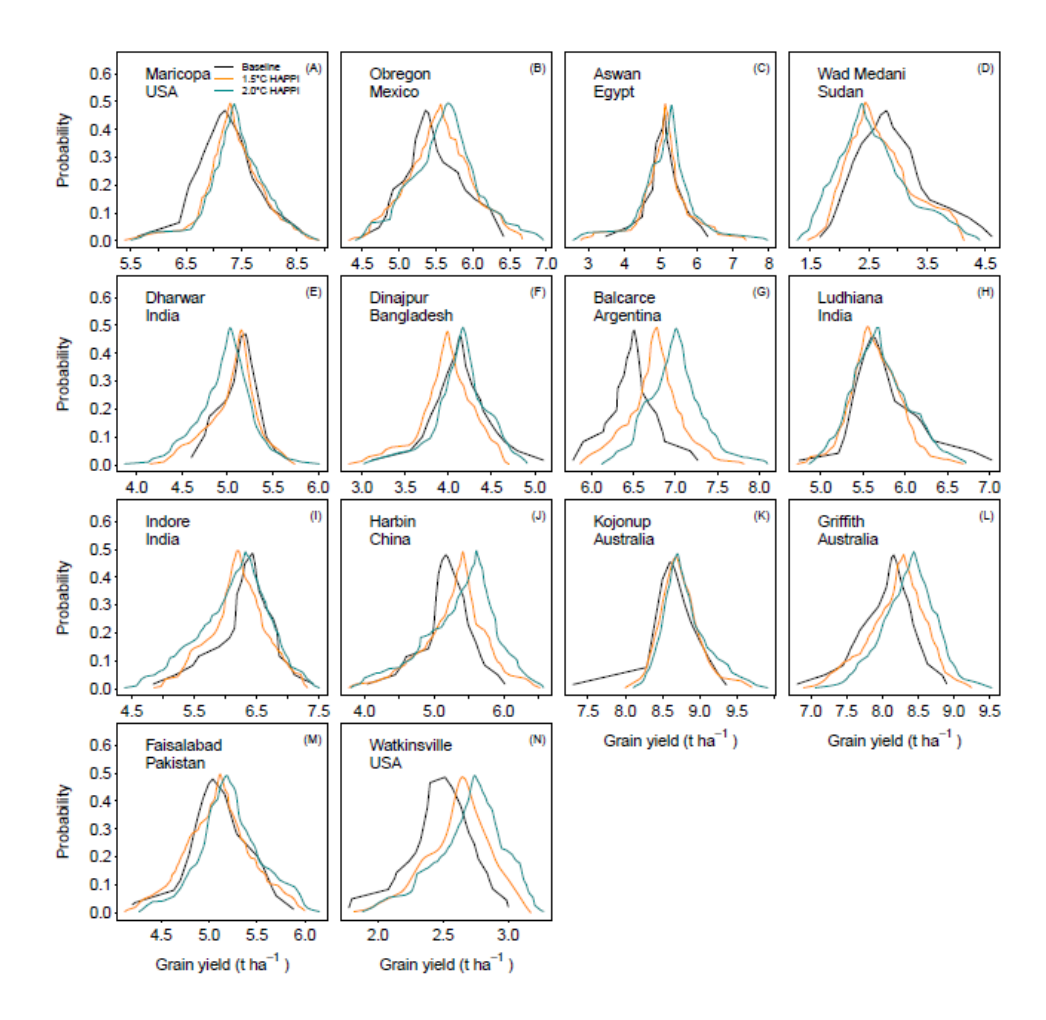


Fig. S12. Yield distribution at 14 hot irrigated global locations for the 1981-2010 baseline and under 1.5 and 2.0 scenarios (including changes in temperature, rainfall and atmospheric CO₂ concentration).



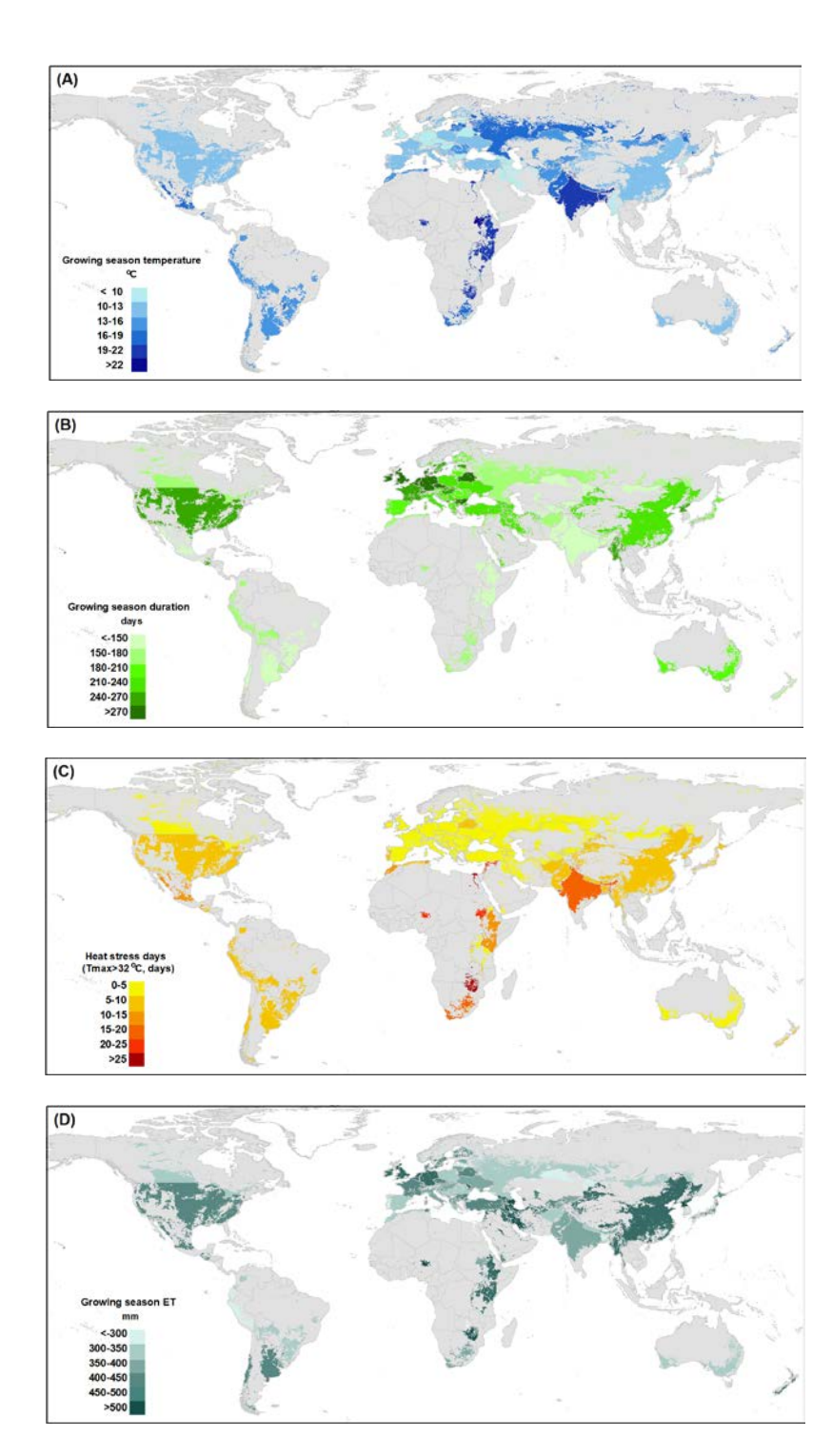
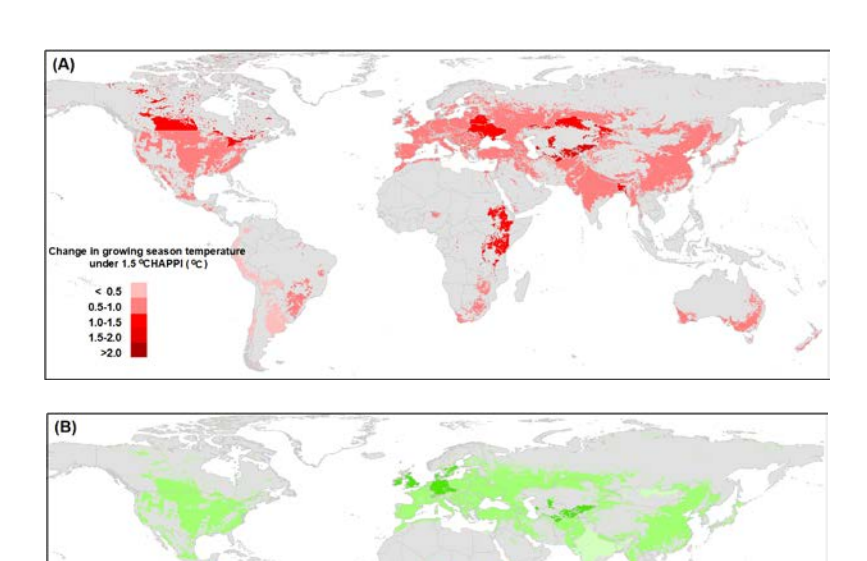
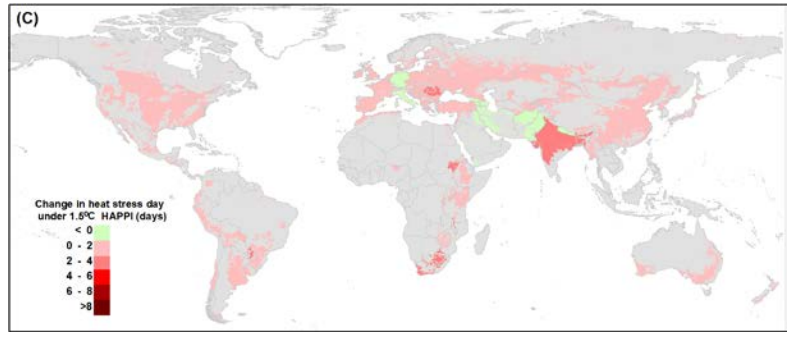


Fig. S13. Simulated multi-model ensemble median of growing season (sowing to maturity) variables by country for the 1981-2010 baseline. (A) Growing season mean temperature. (B) Growing season duration. (C) Heat stress days from anthesis to maturity (daily maximum temperature > 32°C). (D) Growing season evapotranspiration (ET). All growing season variables were calculated from simulated growing season variables at the 60 corresponding locations.







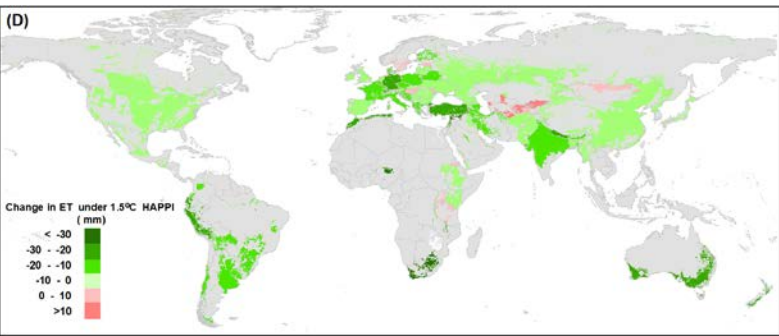


Fig. S14. Simulated multi-model ensemble median of changes in growing season (sowing to maturity) variables by country under 1.5 scenario. (A) growing season mean temperature. (B) Growing season duration. (C) Heat stress days from anthesis to maturity (daily maximum temperature > 32°C). (D) Growing season evapotranspiration (ET). All growing season variables were calculated from simulated growing season variables at the 60 corresponding locations.

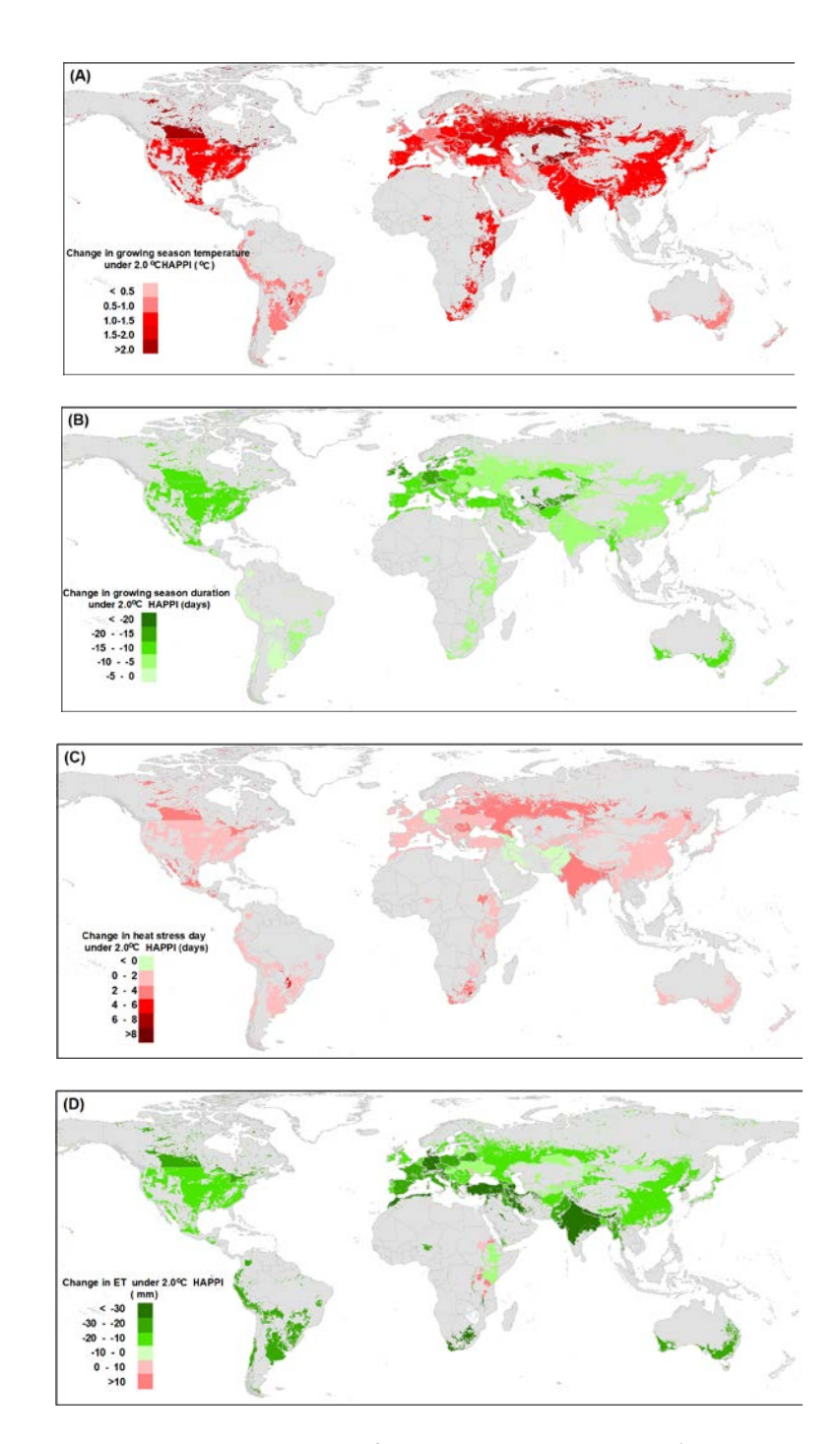


Fig. S15. Simulated multi-model ensemble median of changes in growing season (sowing to maturity) variables by country under 2.0 scenario. (A) growing season mean temperature, (B) growing season duration, (C) heat stress days from anthesis to maturity (daily maximum temperature >32°C), and (D) growing season evapotranspiration (ET). All growing season variables were calculated from simulated growing season variables at the 60 corresponding locations.

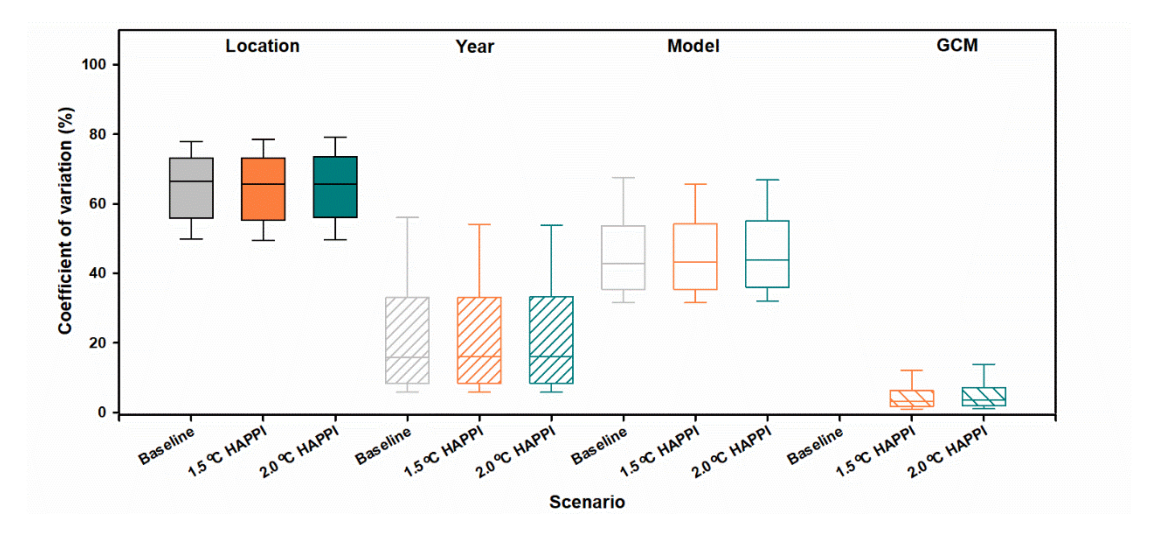


Fig. S16. Coefficient of variation (CV) of simulated wheat grain yields for the 1981-2010 baseline (grey) and 1.5 and (orange) and 2.0 (blue) scenarios. The distribution of CV for 'Location' shows the CVs of simulated wheat grain yields from the 60 global locations within each combination of crop model, year, and GCM. The distribution of CV for 'Year' shows the CVs of simulated wheat grain yields from the 30 years within each combination of crop model, location, and GCM. The distribution of CV for 'Model' shows the CVs of simulated wheat grain yields from the 31 crop models within each combination of location, year, and GCM. The distribution of CV for 'GCM' shows the CVs of simulated wheat grain yields from the five GCMs within each combination of location, crop model, and year. In each box plot, horizontal lines represent, from top to bottom, the 10th percentile, 25th percentile, median, 75th percentile, and 90th percentile of the simulations.

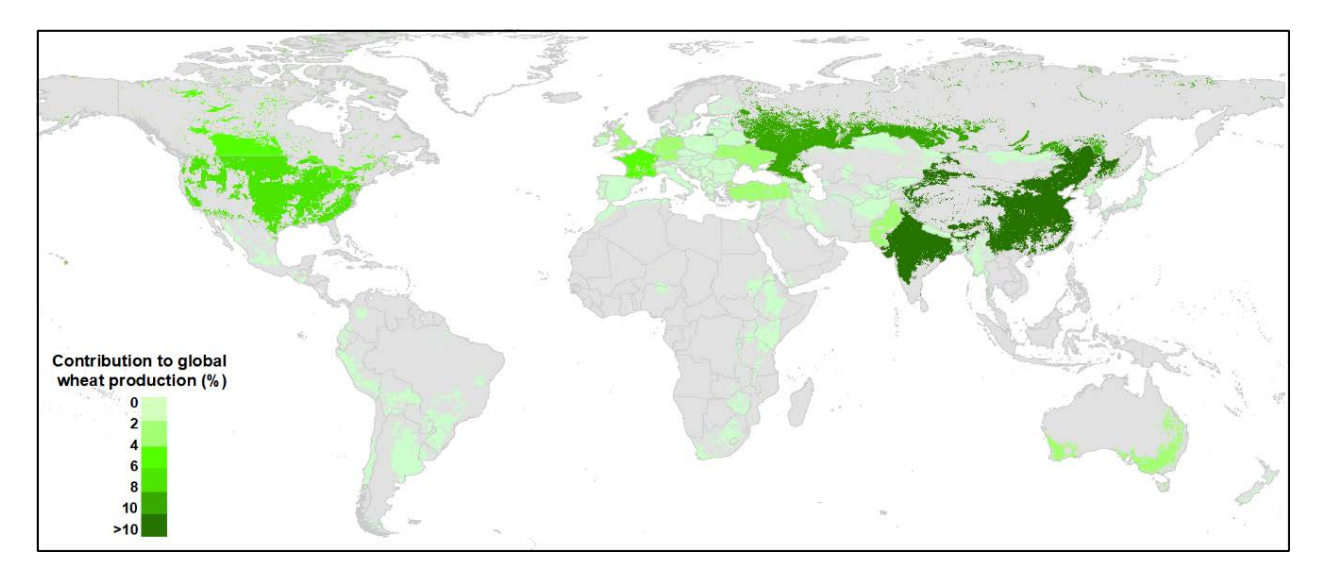


Fig. S17. Contribution of national wheat production from 122 wheat producing countries to global wheat production based on 2014 FAO statistical data.

- 150 1. Asseng S, et al. (2015) Rising temperatures reduce global wheat production. *Nat Clim Change* 5(2):143-147.
- 152 2. Portmann FT, Siebert S, & Döll P (2010) MIRCA2000—Global monthly irrigated and rainfed crop
- areas around the year 2000: A new high resolution data set for agricultural and hydrological modeling. *Global Biogeochemical Cycles* 24(1).
- 155 3. Romero CC, et al. (2012) Reanalysis of a global soil database for crop and environmental modeling. *Environmental Modelling & Software* 35:163-170.
- Gbegbelegbe S, et al. (2017) Baseline simulation for global wheat production with CIMMYT
 mega-environment specific cultivars. Field Crops Research 202:122-135.
- Mitchell D, et al. (2017) Half a degree additional warming, prognosis and projected impacts
 (HAPPI): background and experimental design. Geoscientific Model Development 10(2):571-583.
- Ruane AC, Goldberg R, & Chryssanthacopoulos J (2015) Climate forcing datasets for agricultural
 modeling: Merged products for gap-filling and historical climate series estimation. *Agr Forest Meteorol* 200:233-248.
- 7. FAO (2014) *Asian wheat producing countries-Uzbekistan-Central Zone* (http://www.fao.org/ag/agp/agpc/doc/field/Wheat/asia/Uzbekistan/agroeco_central.htm (last
- 166 visited: 09.22.2015)).
- 167 8. Liu B, et al. (2016) Similar estimates of temperature impacts on global wheat yield by three independent methods. *Nature Clim. Change* 6(12):1130-1136.
- Thao C, et al. (2017) Temperature increase reduces global yields of major crops in four
 independent estimates. Proceedings of the National Academy of Sciences of the United States of
 America 114(35):9326-9331.
- 172 10. R Core Team (2017) R: A language and environment for statistical computing. R Foundation for Statistical Computing. Vienna, Austria. https://www.R-project.org/
- 174 Vienna, Austria.).
- 175 11. Le S, Josse J, & F. H (2008) FactoMineR: An R Package for Multivariate Analysis. *Journal of Statistical Software* 25(1):1-18.
- 177 12. Ramirez-Rodrigues MA, Asseng S, Fraisse C, Stefanova L, & Eisenkolbi A (2014) Tailoring wheat
 178 management to ENSO phases for increased wheat production in Paraguay. *Climate Risk*179 *Management* 3:24-38.
- 13. Asseng S, Travasso MI, Ludwig F, & Magrin GO (2013) Has climate change opened new opportunities for wheat cropping in Argentina? *Climatic change* 117(1-2):181-196.
- 14. Franzluebbers AJ & Stuedemann JA (2014) Crop and cattle production responses to tillage and cover crop management in an integrated crop—livestock system in the southeastern USA. *Eur J Agron* 57:62-70.
- 185 15. Al-Mulla Y, et al. (2009) Soil water and temperature in chemical versus reduced-tillage fallow in a Mediterranean climate. *Applied engineering in agriculture* 25(1):45.
- 187 16. Schillinger WF, Schofstoll SE, & Alldredge JR (2008) Available water and wheat grain yield relations in a Mediterranean climate. *Field Crops Research* 109(1):45-49.
- 189 17. Donaldson E, Schillinger WF, & Dofing SM (2001) Straw production and grain yield relationships in winter wheat. *Crop Science* 41(1):100-106.
- 191 18. Hu W, Schoenau JJ, Cutforth HW, & Si BC (2015) Effects of row-spacing and stubble height on soil water content and water use by canola and wheat in the dry prairie region of Canada.
- 193 Agricultural Water Management 153:77-85.

- 194 19. Izaurralde R, Solberg E, Nyborg M, & Malhi S (1998) Immediate effects of topsoil removal on crop productivity loss and its restoration with commercial fertilizers. *Soil and Tillage Research* 46(3):251-259.
- 197 20. Royo C, *et al.* (2006) Grain growth and yield formation of durum wheat grown at contrasting
 198 latitudes and water regimes in a Mediterranean environment. *Cereal Research Communications*199 34(2-3):1021-1028.
- 21. Steduto P, Pocuca V, Caliandro A, & Debaeke P (1995) An evaluation of the crop-growth simulation submodel of epic for wheat grown in a Mediterranean climate with variable soilwater regimes. *Eur J Agron* 4(3):335-345.
- 203 22. Pecetti L & Hollington P (1997) Application of the CERES-Wheat simulation model to durum wheat in two diverse Mediterranean environments. *Eur J Agron* 6(1):125-139.
- 23. Lithourgidis A, Damalas C, & Gagianas A (2006) Long-term yield patterns for continuous winter wheat cropping in northern Greece. *Eur J Agron* 25(3):208-214.
- 207 24. Berzsenyi Z, Győrffy B, & Lap D (2000) Effect of crop rotation and fertilisation on maize and wheat yields and yield stability in a long-term experiment. *Eur J Agron* 13(2):225-244.
- 209 25. Cuculeanu V, Marica A, & Simota C (1999) Climate change impact on agricultural crops and adaptation options in Romania. *Climate Research* 12(2-3):153-160.
- 211 26. Islam T (1991) Water use of a winter wheat cultivar (Triticum aestivum). *Agricultural Water Management* 19(1):77-84.
- 27. Rötter RP, et al. (2012) Simulation of spring barley yield in different climatic zones of Northern and Central Europe: a comparison of nine crop models. *Field Crops Research* 133:23-36.
- 28. Pavlova VN, Varcheva SE, Bokusheva R, & Calanca P (2014) Modelling the effects of climate variability on spring wheat productivity in the steppe zone of Russia and Kazakhstan. *Ecological Modelling* 277:57-67.
- 218 29. FAO (2010) Asian wheat producing countries-Uzbekistan-Central Zone
- 219 (http://www.fao.org/ag/agp/agpc/doc/field/Wheat/asia/Uzbekistan/agroeco_central.htm (last visited: 09.22.2015)).
- Heng LK, Asseng S, Mejahed K, & Rusan M (2007) Optimizing wheat productivity in two rain-fed environments of the West Asia–North Africa region using a simulation model. *Eur J Agron* 26(2):121-129.
- 224 31. Latiri K, Lhomme J-P, Annabi M, & Setter TL (2010) Wheat production in Tunisia: progress, inter-225 annual variability and relation to rainfall. *Eur J Agron* 33(1):33-42.
- 32. Sommer R, et al. (2012) Simulating the effects of zero tillage and crop residue retention on
 water relations and yield of wheat under rainfed semiarid Mediterranean conditions. Field Crops
 Research 132:40-52.
- Tavakkoli AR & Oweis TY (2004) The role of supplemental irrigation and nitrogen in producing bread wheat in the highlands of Iran. *Agricultural Water Management* 65(3):225-236.
- 34. Ilbeyi A, Ustun H, Oweis T, Pala M, & Benli B (2006) Wheat water productivity and yield in a cool
 highland environment: Effect of early sowing with supplemental irrigation. *Agricultural Water Management* 82(3):399-410.
- 35. Bannayan M, Sanjani S, Alizadeh A, Lotfabadi SS, & Mohamadian A (2010) Association between climate indices, aridity index, and rainfed crop yield in northeast of Iran. *Field Crops Research* 118(2):105-114.
- Iqbal M, et al. (2005) Effect of tillage and fertilizer levels on wheat yield, nitrogen uptake and
 their correlation with carbon isotope discrimination under rainfed conditions in north-west
 Pakistan. Soil and Tillage Research 80(1):47-57.

- Huang G, et al. (2008) Productivity and sustainability of a spring wheat–field pea rotation in a semi-arid environment under conventional and conservation tillage systems. Field Crops
 Research 107(1):43-55.
- 38. Asseng S, et al. (1998) Performance of the APSIM-wheat model in Western Australia. *Field Crop Res* 57(2):163-179.
- van Rees H, et al. (2014) Leading farmers in South East Australia have closed the exploitable wheat yield gap: Prospects for further improvement. *Field Crops Research* 164:1-11.
- 40. Araya T, Nyssen J, Govaerts B, Deckers J, & Cornelis WM (2015) Impacts of conservation
 agriculture-based farming systems on optimizing seasonal rainfall partitioning and productivity
 on vertisols in the Ethiopian drylands. *Soil and Tillage Research* 148:1-13.
- 250 41. Singels A & De Jager J (1991) Determination of optimum wheat cultivar characteristics using a growth model. *Agricultural Systems* 37(1):25-38.
- 42. Keating BA, *et al.* (2003) An overview of APSIM, a model designed for farming systems simulation. *Eur J Agron* 18(3-4):267-288.
- Wang E, et al. (2002) Development of a generic crop model template in the cropping system model APSIM. Eur J Agron 18(1–2):121-140.
- 256 44. Chen C, Wang E, & Yu Q (2010) Modeling Wheat and Maize Productivity as Affected by Climate Variation and Irrigation Supply in North China Plain. *Agronomy Journal* 102(3):1037-1049.
- 258 45. Porter J (1984) A model of canopy development in winter wheat. *The Journal of Agricultural* 259 *Science* 102(02):383-392.
- Weir A, Bragg P, Porter J, & Rayner J (1984) A winter wheat crop simulation model without water or nutrient limitations. *The Journal of Agricultural Science* 102(02):371-382.
- 262 47. Porter JR (1993) AFRCWHEAT2: a model of the growth and development of wheat incorporating responses to water and nitrogen. *Eur J Agron* 2(2):69-82.
- Steduto P, Hsiao T, Raes D, & Fereres E (2009) AquaCrop-The FAO Crop Model to Simulate Yield Response to Water: I. Concepts and Underlying Principles. *Agronomy Journal* 101(3):426-437.
- Stockle C, Donatelli M, & Nelson R (2003) CropSyst, a cropping systems simulation model. Eur J
 Agron 18(3-4):289-307.
- Hoogenboom G & White J (2003) Improving physiological assumptions of simulation models by using gene-based approaches. *Agronomy Journal* 95(1):82-89.
- 270 51. Jones J, et al. (2003) The DSSAT cropping system model. Eur J Agron 18(3-4):235-265.
- 271 52. Ritchie JT, Godwin DC, & Otter-Nacke S (1985) CERES-wheat: A user-oriented wheat yield model.
 272 Preliminary documentation.
- Kassie BT, Asseng A, Porter CH, & Royce F (2016) Performance of DSSAT-Nwheat across a wide
 range of current and future growing conditions. *Field Crops Research* 81:27-36.
- 275 54. Asseng S (2004) *Wheat Crop Systems: A Simulation Analysis* (CSIRO Publishing, Melbourne, Australia) p 275.
- Hunt LA & Pararajasingham S (1995) CROPSIM-wheat a model describing the growth and development of wheat. *Canadian Journal of Plant Science* 75(3):619-632.
- Williams J (1995) The EPIC model in: Computer Models of Watershed Hydrology (Water
 Resources Publications, Highlands Ranch, Colorado, USA).
- 57. Kiniry JR, *et al.* (1995) EPIC model parameters for cereal, oilseed, and forage crops in the northern Great Plains region. *Canadian Journal of Plant Science* 75(3):679-688.
- Williams JR, Jones CA, Kiniry JR, & Spanel DA (1989) The EPIC crop growth model. *Transactions* of the Asae 32(2):497-511.
- Balkovič J, et al. (2014) Global wheat production potentials and management flexibility under the representative concentration pathways. *Global and Planetary Change* 122:107-121.

- Balkovič J, et al. (2013) Pan-European crop modelling with EPIC: Implementation, up-scaling and regional crop yield validation. Agr Syst 120:61-75.
- 289 61. Izaurralde R, Williams JR, McGill WB, Rosenberg NJ, & Jakas MQ (2006) Simulating soil C
 290 dynamics with EPIC: Model description and testing against long-term data. *Ecological Modelling*291 192(3):362-384.
- 292 62. Izaurralde RC, McGill WB, & Williams JR (2012) Development and application of the EPIC model 293 for carbon cycle, greenhouse-gas mitigation, and biofuel studies. *Managing agricultural* 294 *greenhouse gases: Coordinated agricultural research through GRACEnet to address our changing* 295 *climate*, eds Liebig MA, Franzluebbers AJ, & Follett RF (Elsevier, Amsterdam), pp 409-429.
- 296 63. Challinor A, Wheeler T, Craufurd P, Slingo J, & Grimes D (2004) Design and optimisation of a large-area process-based model for annual crops. *Agr Forest Meteorol* 124(1-2):99-120.
- 298 64. Li S, *et al.* (2010) Simulating the Impacts of Global Warming on Wheat in China Using a Large Area Crop Model. *Acta Meteorologica Sinica* 24(1):123-135.
- 300 65. Kersebaum K (2007) Modelling nitrogen dynamics in soil-crop systems with HERMES. *Nutrient Cycling in Agroecosystems* 77(1):39-52.
- Kersebaum KC (2011) Special features of the HERMES model and additional procedures for
 parameterization, calibration, validation, and applications. Ahuja, L.R. and Ma, L. (eds.).
 Methods of introducing system models into agricultural research. Advances in Agricultural
 Systems Modeling Series 2, Madison (ASA-CSSA-SSSA):65-94.
- 306 67. Aggarwal P, et al. (2006) InfoCrop: A dynamic simulation model for the assessment of crop yields, losses due to pests, and environmental impact of agro-ecosystems in tropical environments. II. Performance of the model. *Agricultural Systems* 89(1):47-67.
- Spitters CJT & Schapendonk AHCM (1990) Evaluation of breeding strategies for drought tolerance in potato by means of crop growth simulation. *Plant and Soil* 123:193-203.
- Shibu M, Leffelaar P, van Keulen H, & Aggarwal P (2010) LINTUL3, a simulation model for nitrogen-limited situations: Application to rice. *Eur J Agron* 32(4):255-271.
- Gaiser T, *et al.* (2013) Modeling biopore effects on root growth and biomass production on soils with pronounced sub-soil clay accumulation. *Ecological modelling* 256:6-15.
- Webber H, et al. (2016) Uncertainty in future irrigation water demand and risk of crop failure for maize in Europe. *Environmental Research Letters* 11(7):074007.
- 317 72. Bondeau A, *et al.* (2007) Modelling the role of agriculture for the 20th century global terrestrial carbon balance. *Global Change Biol* 13(3):679-706.
- 319 73. Beringer T, Lucht W, & Schaphoff S (2011) Bioenergy production potential of global biomass 320 plantations under environmental and agricultural constraints. *Global Change Biology Bioenergy* 321 3(4):299-312.
- Fader M, Rost S, Muller C, Bondeau A, & Gerten D (2010) Virtual water content of temperate cereals and maize: Present and potential future patterns. *Journal of Hydrology* 384(3-4):218-231.
- 325 75. Gerten D, Schaphoff S, Haberlandt U, Lucht W, & Sitch S (2004) Terrestrial vegetation and water
 326 balance hydrological evaluation of a dynamic global vegetation model. *Journal of Hydrology* 327 286(1-4):249-270.
- Rost S, et al. (2008) Agricultural green and blue water consumption and its influence on the global water system. Water Resources Research 44(9).
- Müller C, et al. (2007) Effects of changes in CO2, climate, and land use on the carbon balance of
 the land biosphere during the 21st century. Journal of Geophysical Research-Biogeosciences
 112(G2).

- Tao F, Yokozawa M, & Zhang Z (2009) Modelling the impacts of weather and climate variability on crop productivity over a large area: A new process-based model development, optimization, and uncertainties analysis. *Agr Forest Meteorol* 149(5):831-850.
- Tao F, Zhang Z, Liu J, & Yokozawa M (2009) Modelling the impacts of weather and climate variability on crop productivity over a large area: A new super-ensemble-based probabilistic projection. *Agr Forest Meteorol* 149(8):1266-1278.
- Tao F & Zhang Z (2010) Adaptation of maize production to climate change in North China Plain:
 Quantify the relative contributions of adaptation options. *Eur J Agron* 33(2):103-116.
- Tao F & Zhang Z (2013) Climate change, wheat productivity and water use in the North China Plain: A new super-ensemble-based probabilistic projection. *Agr Forest Meteorol* 170(0):146-165.
- Nendel *C, et al.* (2011) The MONICA model: Testing predictability for crop growth, soil moisture and nitrogen dynamics. *Ecological Modelling* 222(9):1614-1625.
- Priesack E, Gayler S, & Hartmann H (2006) The impact of crop growth sub-model choice on simulated water and nitrogen balances. *Nutrient Cycling in Agroecosystems* 75(1-3):1-13.
- Ritchie S, Nguyen H, & Holaday A (1987) Genetic diversity in photosynthesis and water-use efficiency of wheat and wheat relatives. *Journal of Cellular Biochemistry*:43-43.
- 350 85. Biernath C, *et al.* (2011) Evaluating the ability of four crop models to predict different environmental impacts on spring wheat grown in open-top chambers. *Eur J Agron* 35(2):71-82.
- Stenger R, Priesack E, Barkle G, & Sperr C (1999) Expert-N A tool for simulating nitrogen and carbon dynamics in the soil-plant-atmoshpere system. (Land Treatment collective proceedings Technical Session, New Zealand).
- Wang E & Engel T (2000) SPASS: a generic process-oriented crop model with versatile windows interfaces. *Environmental Modelling & Software* 15(2):179-188.
- 357 88. Yin X & van Laar HH (2005) *Crop systems dynamics: an ecophysiological simulation model of genotype-by-environment interactions* (Wageningen Academic Publishers, Wageningen, The Netherlands).
- 360 89. Goudriaan J & Van Laar HH eds (1994) *Modelling Potential Crop Growth Processes. Textbook*361 *With Exercises* (Kluwer Academic Publishers, Dordrecht, The Netherlands), p 238.
- 362 90. Oleary G, Connor D, & White D (1985) A simulation-model of the development, growth and yield of the wheat crop. *Agricultural Systems* 17(1):1-26.
- OLeary G & Connor D (1996) A simulation model of the wheat crop in response to water and nitrogen supply .1. Model construction. *Agricultural Systems* 52(1):1-29.
- OLeary G & Connor D (1996) A simulation model of the wheat crop in response to water and nitrogen supply .2. Model validation. *Agricultural Systems* 52(1):31-55.
- 368 93. Latta J & O'Leary G (2003) Long-term comparison of rotation and fallow tillage systems of wheat in Australia. *Field Crops Research* 83(2):173-190.
- Jamieson P, Semenov M, Brooking I, & Francis G (1998) Sirius: a mechanistic model of wheat response to environmental variation. *Eur J Agron* 8(3-4):161-179.
- 372 95. Jamieson P & Semenov M (2000) Modelling nitrogen uptake and redistribution in wheat. *Field* 373 *Crops Research* 68(1):21-29.
- Handler Sc., Semenov M, & Jamieson P (2005) A wheat canopy model linking leaf area and phenology. *Eur J Agron* 22(1):19-32.
- 376 97. Semenov M & Shewry P (2011) Modelling predicts that heat stress, not drought, will increase vulnerability of wheat in Europe. *Scientific Reports* 1.
- 98. Basso B, Cammarano D, Troccoli A, Chen D, & Ritchie J (2010) Long-term wheat response to
 nitrogen in a rainfed Mediterranean environment: Field data and simulation analysis. *Eur J Agron* 33(2):132-138.

- Senthilkumar S, Basso B, Kravchenko AN, & Robertson GP (2009) Contemporary Evidence of Soil Carbon Loss in the US Corn Belt. *Soil Science Society of America Journal* 73(6):2078-2086.
- 383 100. Angulo *C, et al.* (2013) Implication of crop model calibration strategies for assessing regional impacts of climate change in Europe. *Agr Forest Meteorol* 170:32-46.
- Martre P, et al. (2006) Modelling protein content and composition in relation to crop nitrogen dynamics for wheat. *Eur J Agron* 25(2):138-154.
- Ferrise R, Triossi A, Stratonovitch P, Bindi M, & Martre P (2010) Sowing date and nitrogen fertilisation effects on dry matter and nitrogen dynamics for durum wheat: An experimental and simulation study. *Field Crops Res* 117(2-3):245-257.
- 390 103. He J, Stratonovitch P, Allard V, Semenov MA, & Martre P (2010) Global Sensitivity Analysis of the 391 Process-Based Wheat Simulation Model SiriusQuality1 Identifies Key Genotypic Parameters and 392 Unravels Parameters Interactions. *Procedia - Social and Behavioral Sciences* 2(6):7676-7677.
- 393 104. Maiorano A, *et al.* (2017) Crop model improvement reduces the uncertainty of the response to temperature of multi-model ensembles. *Field Crop Res* 202:5-20.
- Wang E, et al. (2017) The uncertainty of crop yield projections is reduced by improved temperature response functions. *Nat Plants* 3(8):17102.
- 397 106. Soltani A, Maddah V, & Sinclair T (2013) SSM-Wheat: a simulation model for wheat development, growth and yield. *International Journal of Plant Production* 7(4):711-740.
- 399 107. Brisson N, et al. (1998) STICS: a generic model for the simulation of crops and their water and 400 nitrogen balances. I. Theory and parameterization applied to wheat and corn. Agronomie 18(5-401 6):311-346.
- 402 108. Brisson N, et al. (2003) An overview of the crop model STICS. Eur J Agron 18(3-4):309-332.
- 403 109. Cao W & Moss DN (1997) Modelling phasic development in wheat: a conceptual integration of 404 physiological components. *Journal of Agricultural Science* 129:163-172.
- 405 110. Cao W, et al. (2002) Simulating organic growth in wheat based on the organ-weight fraction concept. Plant Production Science 5:248-256.
- 407 111. Yan M, Cao W, & C. Li ZW (2001) Validation and evaluation of a mechanistic model of phasic and phenological development in wheat. *Chinese Agricultural Science* 1:77-82.
- 409 112. Li C, Cao W, & Zhang Y (2002) Comprehensive Pattern of Primordium Initiation in Shoot Apex of Wheat. *ACTA Botanica Sinica* (3):273-278.
- Hu J, Cao W, Zhang J, Jiang D, & Feng J (2004) Quantifying responses of winter wheat
 physiological processes to soil water stress for use in growth simulation modeling. *Pedosphere* 14(4):509-518.
- 414 114. Pan J, Zhu Y, & Cao W (2007) Modeling plant carbon flow and grain starch accumulation in wheat. *Field Crops Research* 101(3):276-284.
- 416 115. Pan J, et al. (2006) Modeling plant nitrogen uptake and grain nitrogen accumulation in wheat. 417 Field Crops Research 97(2-3):322-336.
- Hospital Hamiltonian Hamiltoni